FLUCTUACIÓN DE LA CONCENTRACIÓN ATMOSFÉRICA DE CO_2 DESDE EL PLEISTOCENO TARDÍO AL HOLOCENO MEDIO (15,400 – 4,900 CAL AÑOS AP) Y SU IMPLICACIÓN PARA EL FUNCIONAMIENTO DE NOTHOFAGUS DOMBEY

SEEKING NEW CLUES ON ATMOSPHERIC CO_2 CONCENTRATION FROM THE LATEST PLEISTOCENE TO THE MID-HOLOCENE (15,400 – 4,900 CAL YR BP) AND ITS IMPLICATION FOR NOTHOFAGUS DOMBEY'S PERFORMANCE

Tesis

Entregada A La
Universidad De Chile
En Cumplimiento Parcial De Los Requisitos
Para Optar Al Grado De

Magíster en Ciencias Biológicas

Facultad De Ciencias

Por

Liliana Londoño Ortiz

Abril, 2019

Director de Tesis Dr: Luis Felipe Hinojosa

FACULTAD DE CIENCIAS

UNIVERSIDAD DE CHILE

INFORME DE APROBACION

TESIS DE MAGÍSTER

Se informa a la Escuela de Postgrado de la Facultad de Ciencias que la Tesis de Magíster presentada por la candidata.

Liliana Londoño Ortiz

Ha sido aprobada por la comisión de Evaluación de la tesis como requisito para optar al grado de Magíster en Ciencias Biológicas, en el examen de Defensa Privada de Tesis rendido el día 25 de Marzo de 2019.

Director de Tesis:

Dr. Luis Felipe Hinojosa .....

Comisión de Evaluación de la Tesis

Dra. Alejandra González .....

Dr. Rodrigo Villa .....

RESUMEN BIOGRÁFICO

Liliana Londoño Ortiz
(Amalfi, Antioquia, Colombia)

Bióloga egresada de la Universidad de Antioquia. Su tesis de pregrado consistió en comparar la estructura, diversidad y composición florística en dos fragmentos de bosque secundario expuestos a diferentes perturbaciones antropogénicas, para evaluar la influencia del uso del suelo en el establecimiento y dinámica de las comunidades arbóreas. Después de terminar su pregrado, participó como investigadora asistente en proyectos ecológicos multidisciplinarios enfocados al establecimiento y caracterización de una red de parcelas forestales permanentes, destinadas al monitoreo de la vegetación y el estudio del funcionamiento de los ecosistemas tropicales. Entre el 2011 y 2016, fue pasante en el Instituto Smithsonian de Investigaciones Tropicales (STRI), Panamá. Su investigación se enfocó en el estudio de plantas fósiles del Mioceno (18.1Ma), las cuales utilizó para estimar la concentración atmosférica de CO_2 para este periodo de tiempo, a partir de las características anatómicas de los estomas preservados en las cutículas de hojas fósiles. Actualmente, su investigación se centra en entender los mecanismos que llevaron a la rápida adaptación de *Nothofagus dombeyi* ante los cambios ambientales extremos y a corto plazo durante el último periodo glacial-interglaciar, analizando rasgos anatómicos, morfológicos y fisiológicos de esta especie desde el Pleistoceno tardío (15,300 años) hasta la actualidad.

AGRADECIMIENTOS

Al Laboratorio de Paleoecología, Universidad de Chile. A los proyectos FONDECYT-1150690, Anillo ACT172099 (PIA, Conicyt), AFB170008-IEB, y a la Facultad de Ciencias, Universidad de Chile por el financiamiento brindado.

TABLE OF CONTENTS

LIST OF FIGURES

LIST OF TABLES

RESUMEN

Los cambios climáticos durante los últimos 16,000 años antes del presente (AP: antes del presente), han sido impulsados en gran medida por cambios en la concentración de CO_2 en la atmósfera [CO_2]. El recambio de especies y los cambios en la distribución espacial de las comunidades de plantas, han sido indicadores claves que dan cuenta del efecto de estos cambios sobre las biotas terrestres en el sur de Sur América. Las tendencias globales de las respuestas de las plantas a los cambios de [CO_2] a lo largo del tiempo, han mostrado el impacto de estos sobre las características morfológicas y fisiológicas de las plantas y, a su vez, importantes consecuencias para el funcionamiento de estas. En el presente trabajo, características morfológicas (densidad estomática (SD), tamaño del estoma (SS), longitud del poro (*pl*), y ancho de las células de guardas (*gcw*)) y fisiológicas (conductancia estomática máxima ($g_{c(max)}$), composición isotópica de carbono ($\delta^{13}C$), discriminación isotópica del carbono ($\Delta\delta^{13}C$), la relación entre la concentración de CO_2 intracelular y la concentración de CO_2 en la atmósfera (c_i/c_a)) de muestras fósiles de *Nothofagus dombeyi* fechadas para finales del Pleistoceno tardío (~15,300 – 13,200 cal años AP), y para el Holoceno medio (~6700 – 4900 cal años AP). Adicionalmente, muestras de poblaciones modernas han sido analizadas para determinar los ajustes adaptativos de esta especie a las condiciones ambientes cambiantes desde el

Pleistoceno tardío hasta la actualidad, marcadas por concentraciones contrastantes de CO_2 en la atmósfera.

Se observó una reducción de la SD, *pl*, $g_{c\ (max)}$, $\Delta\delta^{13}C$ y c_i/c_a desde finales del Pleistoceno tardío hasta la actualidad, mientras que el $\delta^{13}C$ mostró una respuesta opuesta; SS y *gcw* no cambiaron a través del tiempo. Las correlaciones entre las características de la hoja revelaron que la variación en $g_{c(max)}$ podría explicarse por los cambios en SD y *pl*, que a su vez se correlacionan con el aumento de las concentraciones de CO_2 en la atmósfera. A través del Pleistoceno tardío y el Holoceno, las poblaciones de *N. dombeyi* experimentaron una atmósfera baja en CO_2, y los ajustes en sus características morfológicas y fisiológicas permitieron a estos individuos superar condiciones adversas, promoviendo su funcionamiento en forma diferente de aquel exhibido por poblaciones modernas expuesta a mayor [CO_2]. La composición del isótopo de carbono de las muestras fósiles y modernas de *N. dombeyi*, ha sido una herramienta importante para comprender los cambios ambientales durante los últimos 15,300 años AP y cómo esta especie se ha adaptado para sobrevivir en ambientes con una disponibilidad de carbono inferior a los niveles actuales.

ABSTRACT

Climatic changes during the last 16,000 years before present (BP: Before present), have been attributed in part to the noteworthy changes of atmospheric CO_2 concentrations [CO_2]. Plant populations turnover, and changes in the spatial distribution of plant communities are the main indicators of the effect of these changes on terrestrial biotas of the southern part of South America. Global trends on plant responses to changes of [CO_2] through time, have shown the impacts of these changes on plant's morphological and physiological characteristics and, in turn, important consequences for plant functioning. Here, morphological (stomatal density (SD), stomatal size (SS), pore length (*pl*), and guard cell width (*gcw*)) and physiological (anatomical maximum stomatal conductance ($g_{c(max)}$), stable carbon isotope ratio ($\delta^{13}C$), carbon isotope discrimination ($\Delta\delta^{13}C$), and the inter-cellular to atmospheric CO_2 ratio (c_i/c_a)) characteristic of fossil samples of *Nothofagus dombeyi* which spanned within the late Pleistocene (~15,300 – 13,200 cal yr BP), and the mid-Holocene (~6,700 – 4,900 cal yr BP), as well as data from modern populations have been analyzed to assess the adaptive adjustments of this species to the novel environments, marked by contrasting concentrations of CO_2 in the atmosphere.

Here, it was observed that SD, *pl*, $g_{c(max)}$, $\Delta\delta^{13}C$, and c_i/c_a, have decreased over the last 15,300 yr BP, while $\delta^{13}C$ showed an opposite response; SS and *gcw* did not change

through time. Correlations between the leaf features reveled that variation in $g_{c(max)}$ could be explained by changes in SD and *pl*, which in turn correlate with the increase of atmospheric CO_2 concentrations. Through late Pleistocene and mid-Holocene, *N. dombeyi* populations underwent a low-CO_2 atmosphere, and adjustments to their morphological and physiological characteristic have lead individuals to come up in this way to defeat adverse conditions, promoting plant functioning different from those of modern population exposed to higher [CO2]. The carbon isotope composition of both fossil and extant *N. dombeyi* samples have been an important tool in understanding the environmental changes since the late Pleistocene, and how *N. dombeyi* has adapted to live in carbon availability lower than current levels.

1 INTRODUCTION

Atmospheric CO_2 concentrations ($[CO_2]$) derived from Antarctic ice core records, show that at the late Pleistocene (between ~20,000 and 17,000 yr BP) CO_2 where to go over ~200 ppm, while at the earliest Holocene (11,700 yr BP), CO_2 levels have reached 270 ppm and remain unvaried throughout pre-industrial time (Figure 1) (Ahn & Brook 2014, Lourantou et al. 2010, Marcott et al. 2014, Monnin et al. 2004, Pépin et al. 2001, Petit et al. 1999, Raynaud et al. 2005, Schmitt et al. 2012). Since then, the concentration of CO_2 in the atmosphere has been risen, and has recently reached its highest level above 400 ppm, a level never seen since about 4.5 million years ago (Pagani et al. 2009, Seki et al. 2010, Keeling et al. 2001, MacFarling Meure et al. 2006). This variation in $[CO_2]$, has been closely associated with the contrasting climatic conditions between the last glacial-interglacial transition, characterized by a prevailing cooler climate and ice-sheet retreat, compared with the nearly constant warm climate at present (Petit et al. 2000). These climatic changes have been determinant in the turnover of terrestrial biotas in the southern part of South America, for example, by limiting the spatial extent range and interaction of plant populations and communities due to a higher ice-covered land mass during the cooler periods, and then, by the altitudinal and poleward expansion as the land is expose due temperature increases (Bennett et al. 2000, Heusser et al. 1999, Moreno & León 2003, Moreno et al. 1999, Villagrán et al. 2004, Villagrán 1995).

Being directly exposed to the environment, plants are useful indicators for assessing both the prevailing ecological and climatic conditions in which these plants developed. Because of this, leaf stomatal characteristics of fossil plants, as well as the diffusive processes involved in the plant carbon uptake, have been the main focus of many paleoclimatic and paleoecological studies (Beerling & Chaloner 1993b, Franks & Beerling 2009, McElwain & Chaloner 1995, Royer 2001, Woodward 1987). Whatever these features are used as proxies to directly or indirectly estimate [CO_2], nearly all studies have consistently demonstrated that changes of [CO_2] have had a significant effect on plant's morphology and physiology through the past. Despite this, the empirical relationship between CO_2 and stomatal features is still challenging, highlighting the importance of incorporating new stomatal-base data.

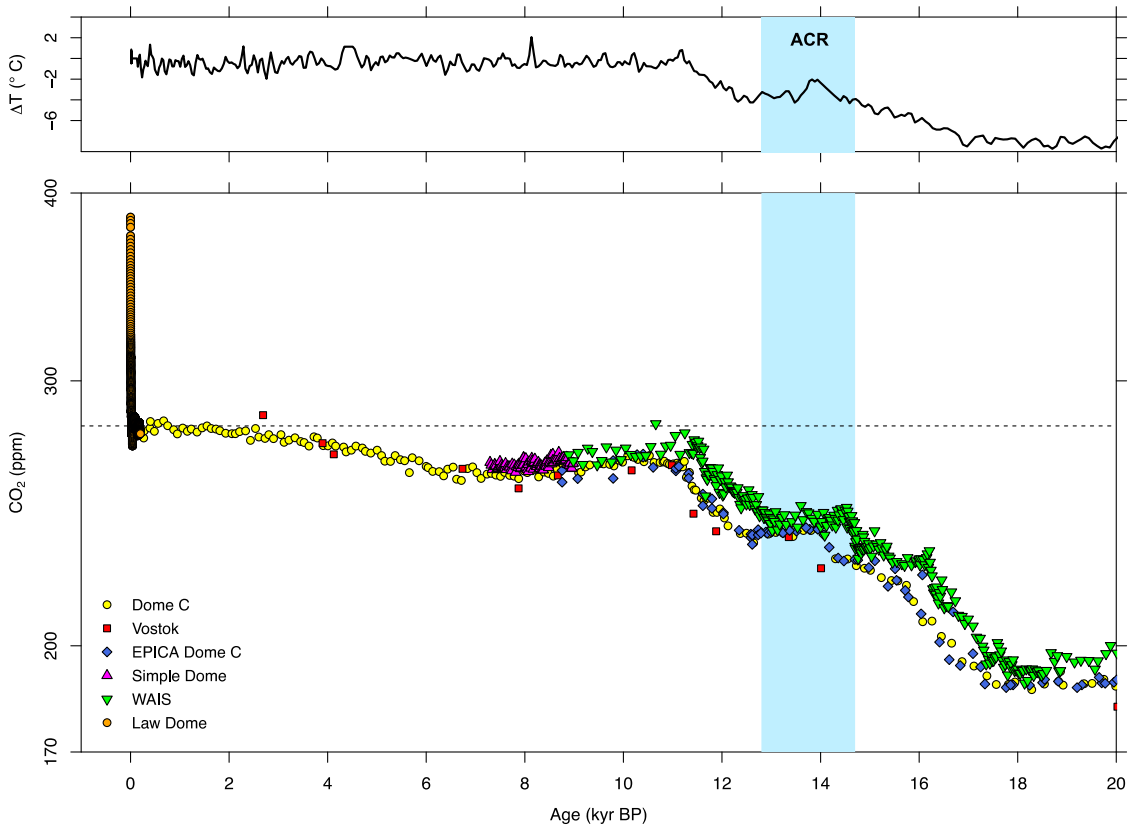

Figure 1. A) Compilation of isotopic (δD) temperature variation from the Vostok Ice Core (Jouzel et al. 1993, Jouzel et al. 1987, Jouzel et al. 1996, Petit et al. 1999). B) Antarctic ice core data of atmospheric CO_2 concentrations from the Dome C ice core (Monnin et al. 2001, Monnin et al. 2004), Vostok (Pépin et al. 2001, Petit et al. 1999, Raynaud et al. 2005), EPICA Dome C (Lourantou et al. 2010, Schmitt et al. 2012), Simple Dome (Ahn & Brook 2014), and WAIS (Marcott et al. 2014). CO_2 data for the past 2000 years are from the Law Dome (Keeling et al. 2001, MacFarling Meure et al. 2006). Horizontal dashed lines represent pre-industrial CO_2 levels. ACR: Antarctic Cold Reversal.

The plants' dependency on atmospheric CO_2 as the main source of carbon for photosynthesis, has been the baseline motivation for several studies carried out to understand the effect of current increases of [CO_2] and the ongoing even highest concentrations of CO_2 on plant physiology, net primary productivity, ecosystems function and stability (Ainsworth & Long 2005, Cernusak et al. 2013, Curtis & Wang 1998, Lloyd & Farquhar 2008, Winter et al. 2001). However, understanding the effect that low [CO_2] have had on plants in the past has received less attention, even though

studies have shown a shocking reduction in the photosynthetic process, growth, and reproduction rates of modern plants grown at lower atmospheric CO_2 levels than they are today (Dippery et al. 1995, Sage & Coleman 2001, Street-Perrott et al. 1997, Ward et al. 2005).

In the Chilean Lake District, late Quaternary macrofossil and microfossil records from the Río Caunahué locality, showed *Nothofagus dombeyi* as the overwhelming dominant species. As part of the cool-temperate North Patagonian rainforest, *N. dombeyi* is associated with Myrtaceae, *Hydrangea*, *Podocarpus nubigena*, and *Saxegothaea conspicua*, at the late Pleistocene (between ~16,000 and 12,000 yr BP). And then, at the mid-Holocene, as part of the thermophilic-angiosperm-forest, associated with *Eucryphia cordifolia, Caldcluvia paniculata, Weinmannia*, and Myrtaceae (Heusser 1981, Markgraf 1991, Markgraf et al. 2002). Today, in Chile, *N. dombeyi* is distributed between 34ºS to 47º S, covering a considerable variation in climatic scenarios, occurring from sea level until about 1800 m.a.s.l, as the dominant canopy species of different plant community assemblies of the Valdivian and North Patagonian rainforests (Zegers 1989, Veblen et al. 1996). Is a light-demanding species, with a high tolerance to drought stress and freezing conditions, high growth rates on canopy gaps or on open site, growing in infertile and well drained sandy soils, and areas characterized by humid and cold conditions (Meza-Basso et al. 1986, Reyes-Díaz et al. 2005, Alberdi 1987). *N. dombeyi* has shown to be a remarkably resilient species since the late Pleistocene, but, what are the mechanisms that have allowed this species to survive through those periods characterized by low [CO_2] and under the higher current levels?

To improves the understanding, and the mechanisms associated of plant responses to the variation of [CO_2], the main purpose of this study was to determine the impact assessment of CO_2 changes on stomata morphological and physiological characteristics of fossil populations of *N. dombeyi* within two particular time periods. The first set of data represent the late Pleistocen (~15,300 – 13,200 cal. yr BP), where cooler climate conditions existed between 14,700 – 12,900 yr BP due to the Antarctic Cold Reversal event (ACR: Pedro et al. 2016), and the second represents the mid-Holocene (~6700 – 4900 cal. yr BP), where also a cooling trend and wetter conditions was observed (Moreno et al. 2018). In addition, a third set of data from modern populations have been integrated to assess the adaptive adjustments of this species to the novel environments from the late Pleistocene to modern time.

Because atmospheric CO_2 changes have influenced how plant communities and ecosystems evolve, here it is hypothesized that the lower [CO_2] during the late Pleistocene and mid-Holocene would be exerting a selective pressure on plant populations of *N. dombeyi*, so that, individuals would have come up with adjustments on the morphological and physiological stomatal characteristics to promote plant functioning under these scenarios, and differed from those of modern population exposed to higher [CO_2].

The specific objectives were the following:

1- To carried out a detailed study of morphological stomatal characteristics (stomatal density, stomatal size, pore length, and guard cell width) among different sets of fossil and modern leaf samples of *N. dombeyi*.

2- To analyzed physiological characteristics (anatomical maximum stomatal conductance ($g_{c(max)}$), carbon isotope composition ($\delta^{13}C$), carbon isotope discrimination ($\Delta\delta^{13}C$), and the inter-cellular to atmospheric CO_2 ratio (c_i/c_a)) among different sets of fossil and modern leaf samples of *N. dombeyi*.

3- To assessed the relationship between the morphological stomatal characteristics, between the physiological characteristics, and between morphological and physiological characteristics.

4- To estimate [CO_2] by implementing a model that relies on the physical mechanism driving air-plant gas exchange (Franks et al., 2014) from late Pleistocene to modern time.

In this study were analyzed 120 fossil leaves deposited in twelve sedimentary facies over a 1.660 cm vertical profile at the outcrop of the Río Caunahué. This outcrop is a sequence of fluvial-lacustrine deposits with a rich paleobotanical record. From each sample, at less 1 mg of leaf tissue was sampled for carbon isotope analysis ($\delta^{13}C$). This analysis was carried out at the Light Stable Isotope Mass Spec Lab in the Department of Geological Sciences at the University of Florida. We used the remaining leaf fragments for the analysis of stomatal characteristics. In order to contrast plant responses to [CO_2], this study compared the fossil features of *N. dombeyi* with those derived from the analysis on leaf litter samples collected at the top of the Caunahué outcrop, as well as from samples collected from sun-exposed branches.

As the [CO_2] keeps getting higher and the expectancy about further responses of plants to the ongoing climate change, there is still a need to improve the understanding of the influence of [CO_2] on plant functioning in the past. It will now be informative to present a detailed analysis of morphological and physiological traits from fossil leaves preserved in sediments from a single site covering the late Pleistocene and mid-Holocene in southern South America, as evidence to infer the processes involved on plant adaptation to the associated climatic changes.

2 METHODS

2.1 Geological setting

The outcrop of the Río Caunahué is located in the western foothill of the Andean Cordillera (40˚7'58.85" S, 72˚14'5.99" W), Región de los Ríos, Chile. This outcrop, is composed of lacustrine and fluvial deposits from the late Pleistocene to Holocene. The fossil plant assemblages are distributed along a stratigraphic sequence that reaches up to 1,660 cm in thickness and approximately 25 fossiliferous horizons can be distinguished. The basal unit consist of multiple successions of laminated gray clays interbedded mostly with dark horizons with high organic matter content. White silts and fine black sandstones were also intermixed between the clays in the upper part of this unit. The middle section is dominated by laminated dark clays, among which are interlaced limes and scarce thin horizons of medium-grain sandstones in the lower part and grey-green clayed mudstone and fine brown layers of mudstone in the upper part. At the top, the section consists of fluvial deposits, predominantly of medium-grain ocher sandstones in sequences which are 20 – 180 cm in thickness, interbedded with slender horizons of organic matter, gray silt and sandy mud deposits (Figure 2).

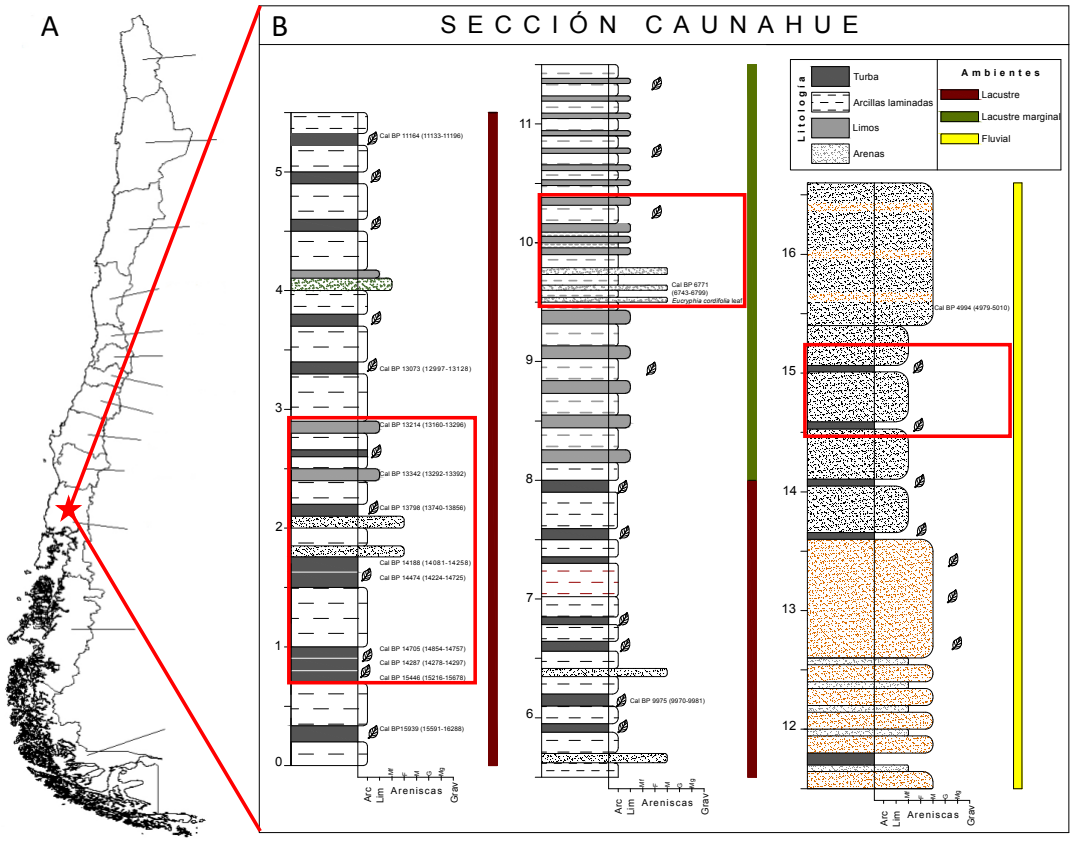

Figure 2. **A**) Map showing the study area location (40˚7'58.85" S, 72˚14'5.99" W) and **B**) Stratigraphic section for the Río Caunahué outcrop, showing the distribution of plant fossil assemblages. In the figure, the twelve layers investigated in this study are indicated by the red squares.

The ages of the boundaries between the different strata are derived from radiocarbon dating in organic remains retrieved from 14 of the 25 horizons. The lower stratum was dated by AMS to 12,990 ± 40 ^{14}C yr BP (15,336 cal. yr BP; CALIB Radiocarbon Calibration Program; Stuiver & Reimer 1993). The upper stratum was dated to 4,460 ± 30 ^{14}C yr BP (4,973 cal. yr BP) (Table 1).

Table 1. Radiocarbon dates of twelve late Pleistocene - Holocene organic sediments from the Río Caunahué outcrop, with range in calendar years BP derived from Calib 3.0 ^{14}C age calibration program.

Nomenclature	Depth (cm)	$\delta^{13}C$ (‰)	^{14}C age	corrected error	1 or 2σ	lower cal range BP	upper cal range BP	Cal BP
BMOV1	59	-31.3	12990	40	1	15215	15678	15336
BMOV2	80	-31.4	12510	40	1	14278	14297	14660
BMOV3	94.5	-30.9	12590	40	1	14654	14757	14837
BMOV4	130	-31.1	12450	40	1	14224	14725	14505
BMOV6	210	-31.1	11940	40	1	13740	13856	13799
BMOV7	250	-31.6	11490	40	1	13292	13392	13333
BMOV8	282	-30.6	11330	40	1	13160	13269	13211
Eucryphya cordifolia	967	-31.3	5960	30	1	6743	6799	6723
BMOVN1	1169	-33.9	4590	30	1	5292	5322	5307
BMOVN2	1198	-31.3	4590	30	1	5292	5322	5161
BMOVN3	1550	-31.3	4460	30	1	4979	5010	4973

2.2 Plant material

2.2.1 Fossil setting

A total of 120 fossil leaves of *N. dombeyi* (10 leaves per facie to ensure a representative sample at each facie) were sampled from twelve stratigraphic horizons in the outcrop of the Río Caunahué. Although depositional beds were not continuously distributed through the length of the stratigraphic column, and break of several thousands of years (from ~13,000 to 7,000 cal. yr BP), *N. dombeyi* spans across all layers.

Late Pleistocene tree assemblages and plant communities were constituted by cold-tolerant species of the southern part of South America, including *N. dombeyi*, and Myrtaceae. While at the mid-Holocene, thermophilous and evergreen species were the representative elements (APPENDIX I). *N. dombeyi* was the most abundant species in each strata analyzed, generally consistent with the palynological data previously reported from the outcrop (Heusser 1981, Markgraf 1991). Paleoclimate data from Río Caunahué macrofossils suggested that mean annual temperatures (MAT) were similar to

the present-day conditions within three time intervals: for the 15,336 -14,188 cal. yr BP interval was 11.4 ± 0.4 ˚C, for the interval between 13,799 - 13,211 cal. yr BP was 12.4 ± 0.45 ˚C, and for the 6,723-4,973 cal. yr BP interval was 13.3 ± 0.5 ˚C (Hinojosa, L. F., Laboratory of Paleoecology, personal observation).

2.2.2 Extant setting

The study was assessed by incorporating data from 10 leaf litter samples, and 10 other modern samples of *N. dombeyi* collected from the upper sun-exposed branches from a rain forest, at the top of the Río Caunahué outcrop. The variation in intrinsic morphological and physiological stomatal traits on modern populations was tested against fossil characteristics to elucidate the mechanisms by which this species responds to changes on [CO_2]. The mean annual temperature (MAT) and mean annual precipitation (MAP) of the site are 12ºC and 2559 mm respectively (Figure 3; data from Lago Ranco (DGA:10307001) and Lago Maihue (DGA:10304002) meteorological stations, located 31.5 and 12.8 kilometers from the Río Caunahué outcrop, respectively; in Los Ríos Region from 2000 to 2016).

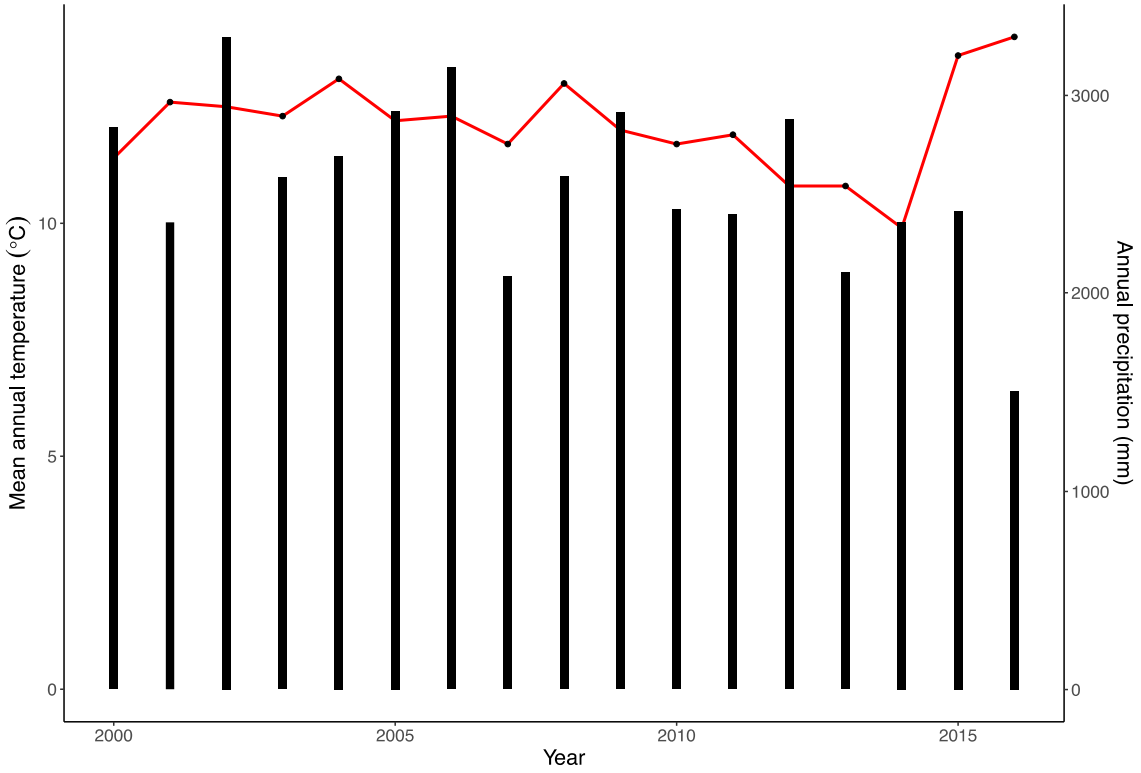

Figure 3. Climatic data from Lago Ranco (DGA:10307001) and Lago Maihue (DGA:10304002) climate stations for the Río Caunahué locality sampled.

2.2.3 Cuticle preparation

Both fossil and modern leaves were bleached with sodium hypochlorite (4.9%), from one up to three days. After the leaves turned white, they were rinsed with tap water, and then dehydrated in solutions of ethanol at increasing concentrations of 50%, 75%, and 96% for five minutes each treatment. After dehydration, leaf samples were stained in a safranin solution and stored under 20% ethanol. The stained leaf samples were then mounted in water on microscopic slides, and examined using a ZEISS Axio Lab. A1 light microscope (Figure 4).

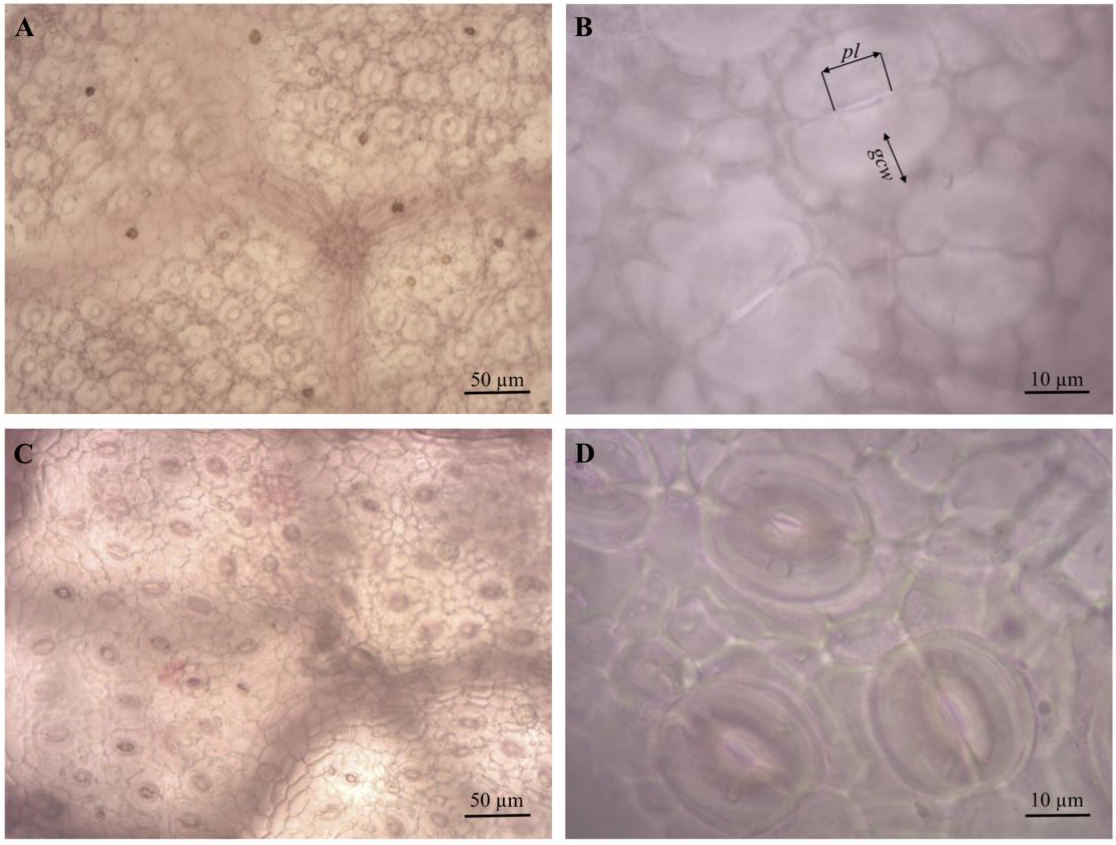

Figure 4. Images of cleared cuticles of *Nothofagus dombeyi* from the Rio Caunahué outcrop showing a field of view for SD counting, and stomatal morphological measurements (pore length: *pl* and guard cell width: *gcw*) of a 15. 336 years' fossil sample **(A)** and **(B)**; and a modern leaf sample **(C)** and **(D).**

2.3 Analysis of morphological and physiological characteristics

Stomatal density (SD, number of stomata per mm^2 [n/mm^2]) was counted using an image-processing program (ImageJ) from seven digital images taken using an Axio Lab. A1 at 200x of magnification. Stomatal pore length (*pl*), and single guard cell width (*gcw*) were measured using ImageJ from digital images of 10 stomata taken at 1000x of magnification (Figure 4B). From these measurements, anatomical maximum stomatal conductance to water vapor ($g_{w(max)}$) was calculated by following the equation of Franks and Beerling (2009):

$$g_{w(max)} = \frac{\frac{\mathrm{dw}}{v} \cdot \mathrm{SD} \cdot pa_{max}}{pd + \frac{\pi}{2}\sqrt{pa_{max}/\pi}}$$

where *dw* is diffusivity of water vapour at 25ºC (0.0000249 m^2s^{-1}), *v* is the molar volume of air (0.0224 m^3mol^{-1}), SD the stomatal density (m^{-2}), pa_{max} the maximum stomatal pore area (m^2) (calculated as the area of an ellipse, using *pl* as the semi-major axis and $^{pl}/_2$ as the semi-minor axis), and *pd* is the stomatal pore depth (m) (equivalent to the width of a single guard cell). Then, the maximum stomatal conductance to CO_2 ($g_{c(max)}$) can be calculated by dividing $g_{w(max)}$ by the ratio H_2O diffusion/CO_2 diffusion in air (1.6; Farquhar et al. 1989, Lambers et al. 1998).

Analysis of stable carbon isotope composition ($\delta^{13}C$) of each leaf sample is an important feature to estimate inter-cellular to atmospheric CO_2 ratio (c_i/c_a). Between 0.5 mg up to 1.3 mg of fossil and fresh samples were loaded into tin sample capsules and placed in a 50-position automated carousel on the Carlo Erba NA1500 elemental analyzer. Combustion gases were carried in a helium stream through a Conflo II interface to a Thermo Delta V Plus isotope ratio mass spectrometer. All carbon isotope results are expressed in standard delta notation relative to the Vienna Pee Dee Belemnite (VPDB). c_i/c_a was obtained following the equations of Farquhar et al. (1989).

First, the carbon isotope discrimination (Δ) is calculated as:

$$\Delta_{\text{leaf}} = \frac{\boldsymbol{\delta}^{13}C_{\text{air}} - \boldsymbol{\delta}^{13}C_{\text{leaf}}}{1 + \boldsymbol{\delta}^{13}C_{\text{leaf}}/1000}$$

where $\delta^{13}C_{air}$ is the carbon isotope composition of the atmosphere, $\delta^{13}C_{leaf}$ is the carbon isotope composition of the leaf tissue. Here, $\delta^{13}C_{air}$ values for the late Pleistocene and mid-Holocene, were taken from Eggleston et al. (2016). Modern $\delta^{13}C_{air}$ values were taken from Mauna Loa (http://www.esrl.noaa.gov/gmd/ccgg/trends).

then, c_i/c_a can be calculated as:

$$c_i/c_a = \frac{\Delta_{\text{leaf}} - a}{b - a}$$

where a is the fractionation due to slower diffusion of $^{13}CO_2$ relative to $^{12}CO_2$ (4.4‰), and b the fractionation caused by discrimination effects of Rubisco (30‰).

also, c_i can be derive from $\delta^{13}C$ as:

$$c_i = c_a \left(\frac{\Delta_{\text{leaf}} - a}{b - a} \right)$$

where c_a is the atmospheric CO_2 concentration, Δ_{leaf} is the carbon isotope discrimination, a the fractionation due to slower diffusion of $^{13}CO_2$ relative to $^{12}CO_2$ (4.4‰), and b the fractionation caused by discrimination effects of Rubisco (30‰).

2.4 CO_2 estimations

In this study, the photosynthetic-model approach proposed by Franks et al. (2014) to estimate [CO_2] was applied. This model relies on the physical mechanism driving air-plant gas exchange during the photosynthetic process. It assumes plant physiological functioning under certain conditions of [CO_2], and its effect on the rate of carbon assimilation (A_n) in relation to the total operational conductance to CO_2 diffusion from the atmosphere to inside the leaf ($g_{c(tot)}$), and the ratio of CO_2 concentration inside the leaf (c_i) to the CO_2 concentration in the atmosphere (c_a) (c_i/c_a) (Farquhar & Sharkey 1982, Von Caemmerer 2000).

$$c_a = \frac{A_n}{g_{c(tot)} \times (1 - c_i / c_a)}$$

The rate of carbon assimilation (A_n) cannot be estimate from fossils material, and was therefore obtained from empirical studies on gas exchange in plants of *N. dombeyi*. The photosynthetic rate at a known [CO_2] (*A0)* was taken as 11.4 μmol m^{-2} s^{-1}, a value under typical field conditions in the growing season (Lusk et al. 2003). As defined by Franks et al. (2014), here, the previously set of equations describing the dynamics of the plant physiological functioning was append to the model, so that the model can be solved and applied to the fossil assemblages using the R code designed for the model (Franks et al. 2014).

Through Monte Carlo simulation, all input parameters were resampled 10.000 of times. The estimated CO_2 value for each time of interest, was obtained as the median value of the simulation results.

2.5 Statistical analysis

Each stomatal trait value was taken as the arithmetic mean of the ten leaves sampled per layer. In order to assess the distribution of all of the variables, the data were checked for normality using the inferential test of normality Shapiro-Wilk's W test and for homoscedasticity using levene's Test in the packages dplyr and car in R (Wickham et al. 2017, Fox & Weisberg 2011). Where necessary, data were transformed to improve normality and homoscedasticity of the variance using the log10 transformation. The analysis of variance (ANOVA) with Tukey's post-hoc test was used to examined for significant differences between sets of data in the mean morphological and physiological stomatal characteristics. Furthermore, a correlation analysis was performed to assess the relationship within and between morphological and physiological characteristics using the Pearson product-moment method on $\log_{10}$ transformed data.

3 RESULTS

3.1 Morphological and physiological characteristics through time

The morphological and physiologic characteristics for the 140 samples studied are presented in Appendix II. Mean stomatal densities (SD ± standard deviation) of the late Pleistocene, mid-Holocene fossils, and modern leaves of *N. dombeyi* were 436 ± 64, 434 ± 74 and 353 ± 40 mm^{-2}, respectively. No differences were found when considering CO_2 responses neither within the late Pleistocene ($P > 0.05$ for $_{log10}$ transformed values) nor within the mid-Holocene samples ($P > 0.05$ for log10 transformed values), or between them ($P > 0.05$ for log_{10} transformed values). Moreover, there is a statistically significant difference between mean SD values of *N. dombeyi* samples from the late Pleistocene and modern ($P < 0.0001$ for log_{10} transformed values), as well as difference between mid-Holocene and modern samples ($P < 0.0001$ for log_{10} transformed values) (Figure 5A). There are not differences in SS within or between the three epochs analyzed ($P > 0.05$ for log10 transformed values) (Figure 5B). The stomatal *pl* differed significantly across epochs ($P < 0.002$ for log_{10} transformed values), with longer *pl* in the late Pleistocene samples (9.7 ± 0.7 μm) and shorter *pl* in modern samples (8.2 ± 0.4 μm) (Figure 5C). No differences were found for *gcw* within or between the three epochs analyzed ($P > 0.05$ for log_{10} transformed values) (Figure 5D).

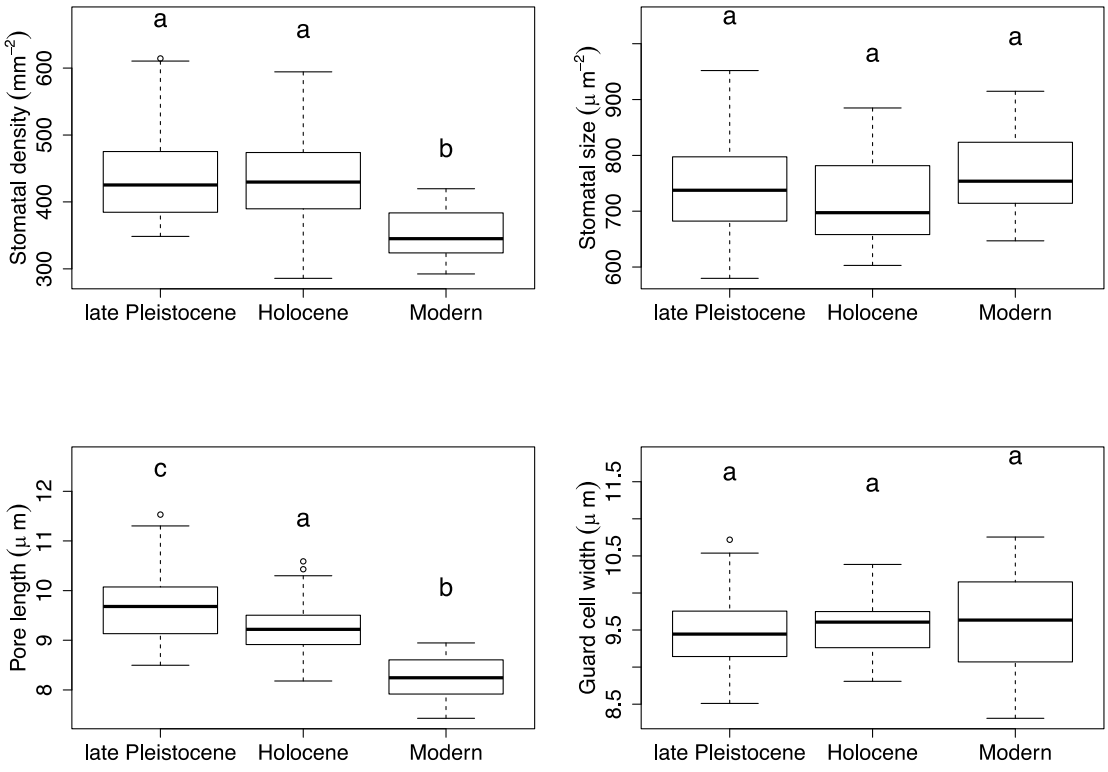

Figure 5. Boxplots of morphological stomatal characteristic of *Nothofagus dombeyi* samples from the late Pleistocene (~15,300 – 13,200 ^{14}C yr BP), mid-Holocene (~6,700 – 4,900 ^{14}C yr BP), and modern time. **(A)** stomatal density (SD), **(B)** stomatal size (SS), **(C)** pole length (*pl*), and **(D)** guard cell width (*gcw*). Different letters indicate significant differences between epochs (P<0.05).

The relationship between SD and SS was significant and negative across the three epochs studied (late Pleistocene: r = -0.584, P < 0.0001; mid-Holocene: r = -0.463, P < 0.003; modern: r = -0.629, P < 0.003) (Figure 6A). Negative correlation was also showed between SD and *pl* (late Pleistocene: r = -0.272, P < 0.01; mid-Holocene: r = -0.229, P> 0.05; modern: r = -0.258, P > 0.05) (Figure 6B). SD of the late Pleistocene and Holocene samples showed weak negative relationship with *gcw* (r = -0.170, P = 0.1, r = -0.130, P = 0.4; respectively), while in modern samples was significant and negative (r = -0.589, P < 0.01) (Figure 6C).

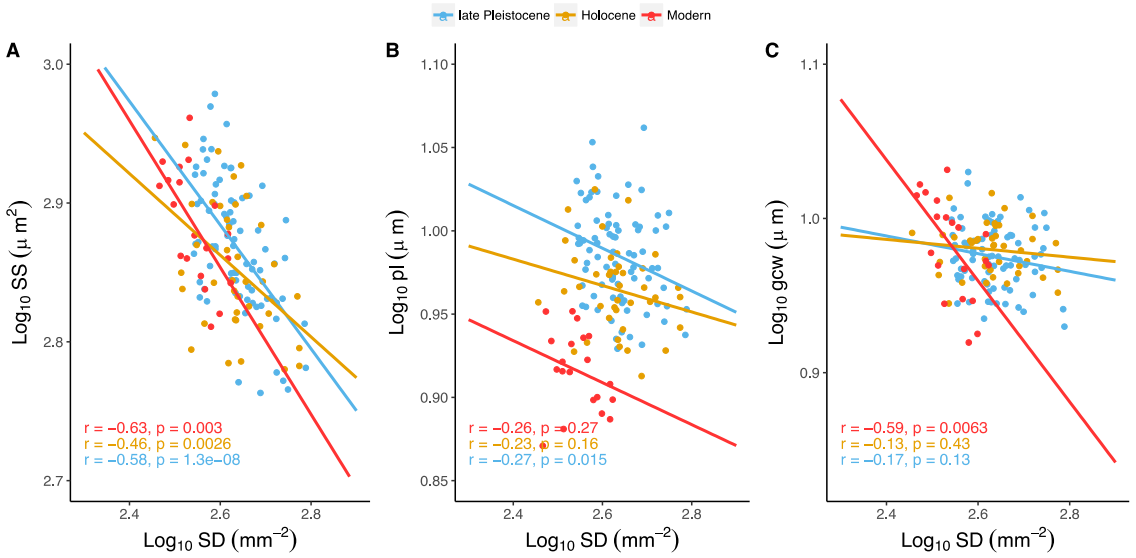

Figure 6. Log-log plots of stomatal density (SD) against **(A)** stomatal size (SS), **(B)** pore length (*pl*), and **(C)** guard cell width (*gcw*) of *Nothofagus dombeyi* samples from the late Pleistocene (~15,300 – 13,200 ^{14}C yr BP), mid-Holocene (~6,700 – 4,900 ^{14}C yr BP), and modern time.

There is a significant decrease of $g_{c(max)}$ values since the late Pleistocene (1.10 ± 0.17, 1.03 ± 0.18 and 0.69 ± 0.09 mol m^{-2} s^{-1}; respectively). Although no significant differences were found between $g_{c(max)}$ values of the late Pleistocene and mid-Holocene samples (P > 0.05 for log$_{10}$ transformed values), there were significant differences between the late Pleistocene and modern samples (P < 0.0001 for log$_{10}$ transformed values), and between mid-Holocene and modern samples (P < 0.0001 for log$_{10}$ transformed values) (Figure 7A). *N. dombeyi* has shown a wide range of variation of isotopic composition, the maximum range was up to ~5‰ in all time intervals. The late Pleistocene leaf samples were isotopically depleted with the heavier ^{13}C isotope (-29.45 ± 1.07‰), while those from the mid-Holocene and modern samples were relatively enriched in the heavier ^{13}C isotope (-28.56 ± 1.08 and -28.23 ± 1.78 ‰; respectively). From the late Pleistocene to mid-Holocene, δ^{13}C became 0.88‰ less negative, which

represent a significant change from one epoch to another ($P < 0.001$ for log10 transformed values), and from the mid-Holocene to present days it rises up 0.33‰ more (Figure 7B), increase that does not make a significant difference between them ($P > 0.05$ for $\log_{10}$ transformed values). There were significant differences between mean carbon discrimination values ($\Delta\delta^{13}C$) of the late Pleistocene, mid-Holocene, and modern samples (23.65 ± 1.13, 22.71 ± 1.14 and 20.31 ± 1.87‰, respectively; $P < 0.001$). No significant differences in $\Delta\delta^{13}C$ values were found within the three epochs analyzed ($P > 0.05$ for $\log_{10}$ transformed values) (Figure 7C). The isotope-based estimates of c_i/c_a ratios differed significantly between the three epochs analyzed (0.75 ± 0.04, 0.72 ± 0.04 and 0.62 ± 0.07, respectively; $P < 0.001$) (Figure 7D).

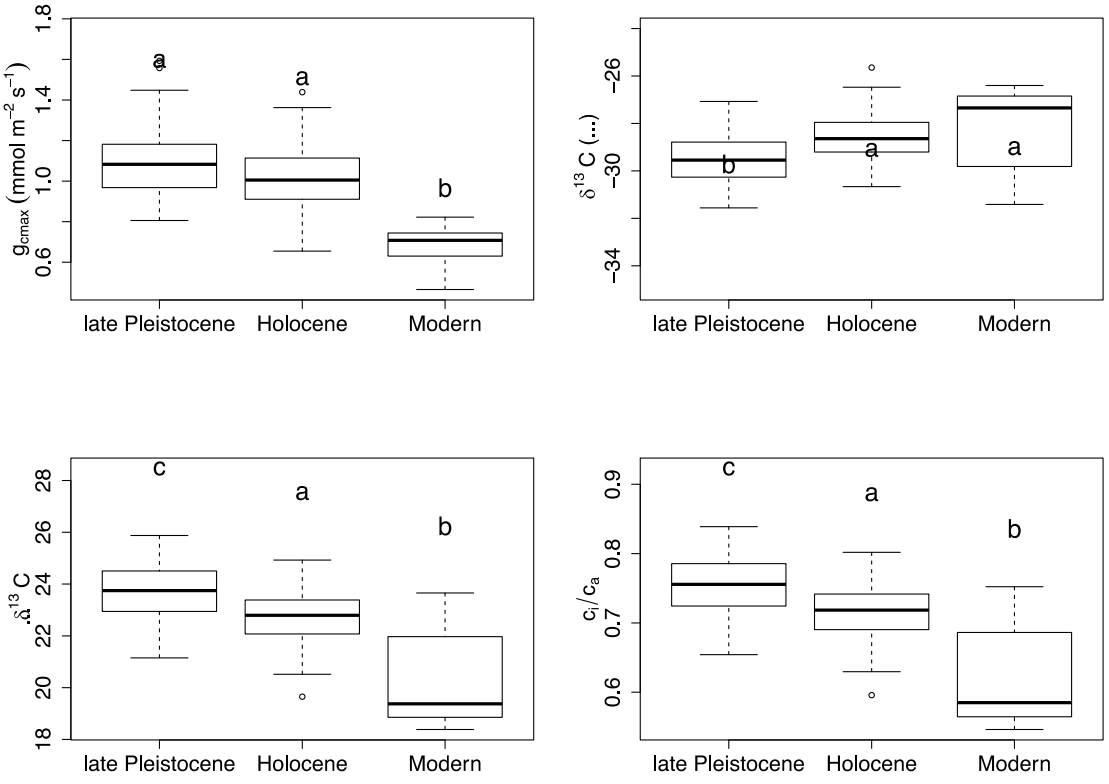

Figure 7. Boxplots of physiological characteristic of *Nothofagus dombeyi* samples from the late Pleistocene (~15,300 – 13,200 ^{14}C yr BP), mid-Holocene (~6,700 – 4,900 ^{14}C yr BP), and modern time.

(A) stomatal conductance, **(B)** carbon isotope composition, **(C)** net isotopic discrimination, and **(D)** *ci/ca* ratio. Different letters indicate significant differences between epochs (P<0.05).

The leaf nitrogen content (%) increased from the late Pleistocene to modern time (0.54 ± 0.22, 0.76 ± 0.32, 1.18 ± 0.67, respectively), and differed significantly between the three epochs analyzed ($P < 0.003$ for $\log_{10}$ transformed values) (Figure 8A). The c_i value was strongly depleted in sample leaves from the late Pleistocene and increased to higher values in the mid-Holocene and modern samples (173 ± 10 ppm, 193 ± 12 ppm, and 244 ± 26 ppm; respectively) (Figure 8B). And, differ significantly among the three epochs studied ($P < 0.001$, for $\log_{10}$ transformed data). These changes in c_i values of *N. dombeyi* leave since the late Pleistocene, negatively correlated with SD ($P < 0.001$), and *pl* ($P < 0.001$).

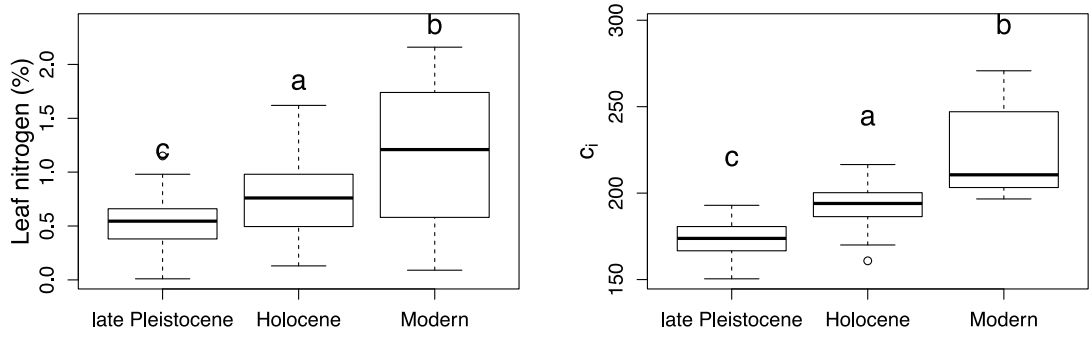

Figure 8. Boxplots of the variation of **(A)** leaf nitrogen content, and **(B)** leaf intercellular CO_2 concentration of *Nothofagus dombeyi* samples from the late Pleistocene (~15,300 – 13,200 ^{14}C yr BP), mid-Holocene (~6,700 – 4,900 ^{14}C yr BP), and modern time. Different letters indicate significant differences between epochs (P<0.05)

3.2 Relationship between morphological and physiological characteristics

The relationship between SD and $g_{c(max)}$ has a strong positive correlation in the three time epochs (SD-$g_{c(max)}$: late Pleistocene $r = 0.751$; $P < 0.0001$, mid-Holocene $r = 0.852$;

$P < 0.0001$, modern $r = 0.806$; $P < 0.0001$, Figure 9A). A positive correlation also was found between *pl* and $g_{c(max)}$ (late Pleistocene $r = 0.375$; $P < 0.001$, mid-Holocene $r = 0.262$; $P > 0.05$, modern $r = 0.226$; $P > 0.05$, Figure 9B). No relationship between *gwc* and $g_{c(max)}$ was found within the late Pleistocene ($r = -0.051$; $P = 0.651$), or mid-Holocene samples ($r = 0.0051$; $P = 0.972$). However, *gcw* correlated negatively with $g_{c(max)}$ within modern samples ($r = -0.519$; $P = 0.02$) (Figure 9C). Negative correlation was showed between $g_{c(max)}$ and SS within all three different epochs (late Pleistocene $r = -0.318$; $P < 0.01$, mid-Holocene $r = -0.240$; $P = 0.1$, Modern $r = -0.458$; $P < 0.05$, Figure 9D).

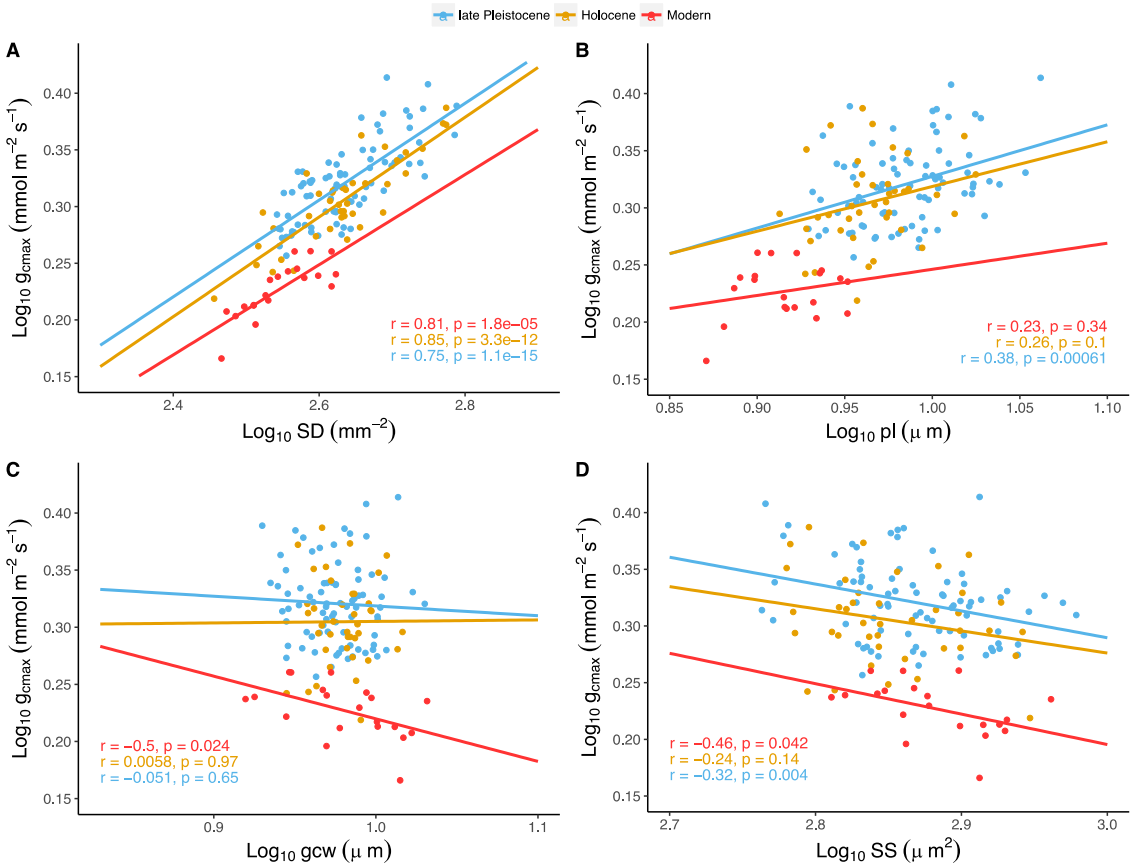

Figure 9. Log-log plots of maximum stomatal conductance ($g_{c(max)}$) against **(A)** stomatal density, **(B)** pore length, **(C)** guard cell width, and **(D)** stomatal size of *Nothofagus dombeyi* samples from the late Pleistocene (~15,300 – 13,200 ^{14}C yr BP), mid-Holocene (~6,700 – 4,900 ^{14}C yr BP), and modern time.

No clear relationship was found between $g_{c(max)}$ and physiological stomatal characteristics ($\delta^{13}C$, $\Delta\delta^{13}C$, *ci/ca* ratio, and c_i). For example, within the late Pleistocene samples, $g_{c(max)}$ was not correlated with $\delta^{13}C$ (r = -0.098; $P > 0.05$), however, were positively correlated in the mid-Holocene (r = 0.378; $P < 0.05$), and negatively correlated within modern samples (r = -0.523; $P < 0.05$) (Figure 10A). $g_{c(max)}$ values of the late Pleistocene samples were not correlated to $\Delta\delta^{13}C$ (r = 0.09; $P > 0.05$), but were negatively correlated to $\Delta\delta^{13}C$ within mid-Holocene samples (r = -0.378; $P < 0.05$ 0.05), and positively correlated to $\Delta\delta^{13}C$ within modern samples (r = 0.523; $P < 0.05$) (Figure

10B). $g_{c(max)}$ and *ci*/*ca* ratio were not correlated within the late Pleistocene samples (r = 0.098; $P > 0.05$), whereas the same variables were negatively correlated within mid-Holocene samples (r = -0.378; $P < 0.05$), and positively correlated in modern samples (r = 0.524; $P < 0.05$) (Figure 10C). $g_{c(max)}$ and *ci* were not correlated within the late Pleistocene samples (r = 0.097; $P > 0.05$), negatively correlated within mid-Holocene samples (r = -0.377; $P < 0.05$), and positively correlated in modern samples (r = 0.522; $P < 0.05$) (Figure 10D).

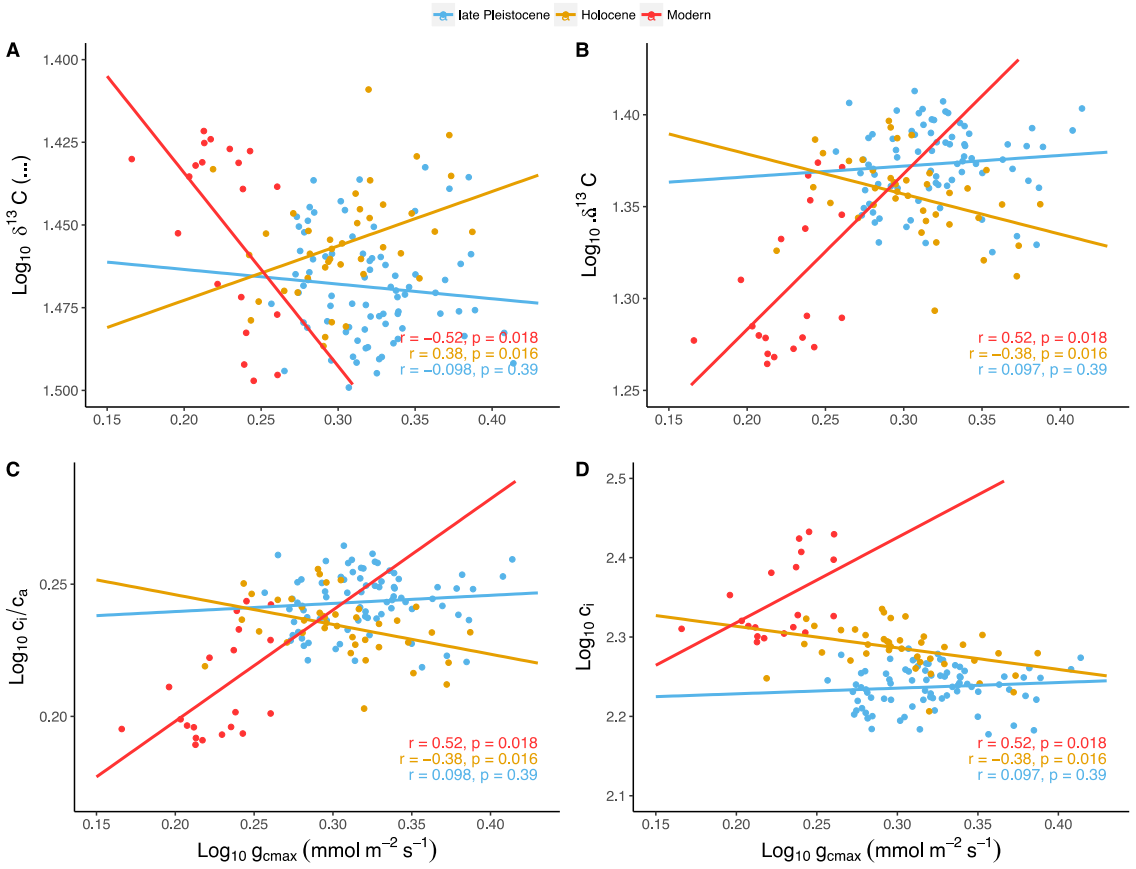

Figure 10. Log-log plots of maximum stomatal conductance ($g_{c(max)}$) against **(A)** carbon isotope composition ($\delta^{13}C$), **(B)** net isotopic discrimination ($\Delta\delta^{13}C$), **(C)** c_i/c_a ratio and **(D)** leaf internal CO_2 concentration (c_i) of *Nothofagus dombeyi* samples from the late Pleistocene (~15,300 – 13,200 ^{14}C yr BP), mid-Holocene (~6,700 – 4,900 ^{14}C yr BP), and modern time.

3.3 CO_2 estimations

The estimated median value of CO_2 using modern *N. dombeyi* samples was 487 ppm, with a range of fluctuation between 318 and 803 ppm. Abrupt CO_2 changes have been observed from the late Pleistocene estimated values. CO_2 concentration by 15,336 year BP was 560 ppm, followed by an increase in CO_2 levels by 14,837 year BP (649 ppm), then, CO_2 decline to 598 ppm by 14,660 year BP, prior to a marked increase in CO_2 by 14,188 years BP (679 ppm) and then, another decline to 13,799 year BP (546 ppm) followed by a marked rice of CO_2 levels at 13,333 years BP (656ppm), followed by a fall in CO_2 by 13,211 years BP (548ppm). At the mid-Holocene, median value of CO_2 was 544 ppm, estimated CO_2 levels from 6,723 to 5,161 years BP rise from 519 to 603 ppm, followed by a fall by 4,973 (523 ppm) (Figure 11).

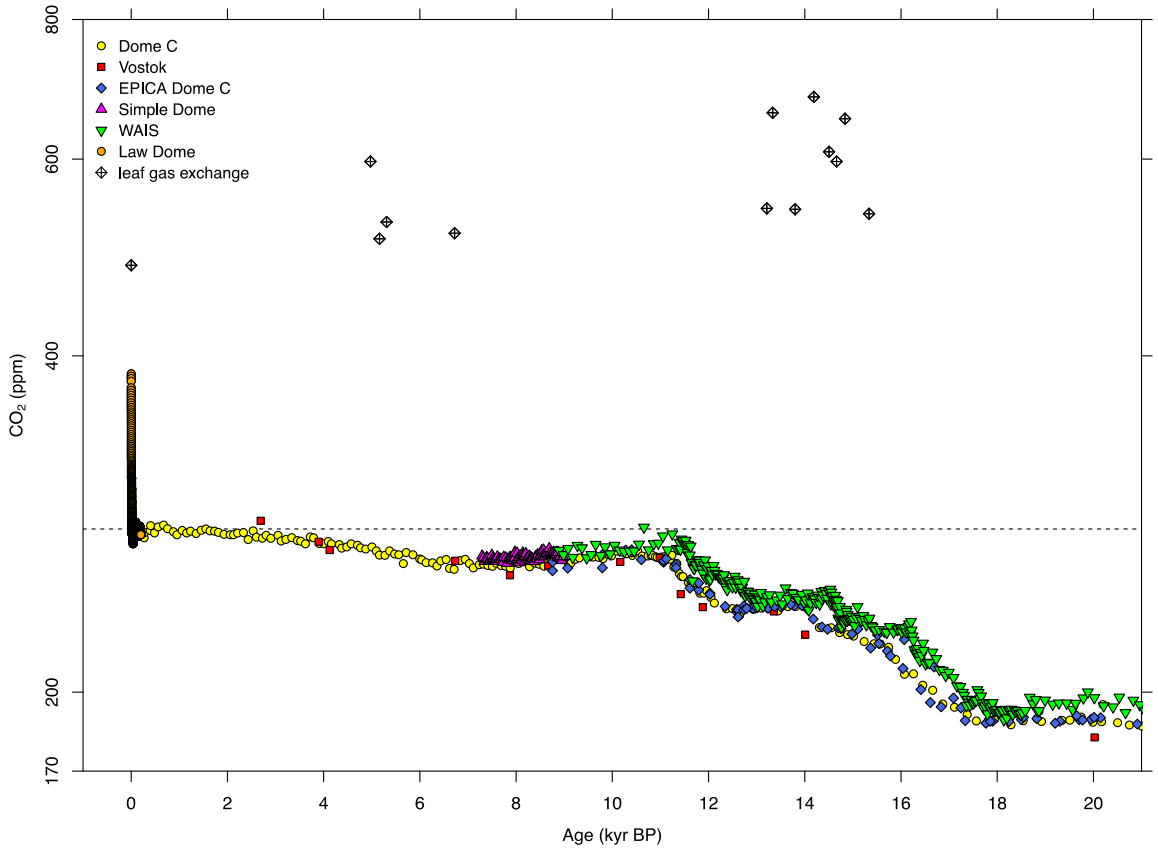

Figure 11. Late Pleistocene and mid-Holocene CO_2 estimates from fossil and modern leaf samples of *Nothofagus dombeyi* from the Río Caunahué outcrop, and Antarctic ice core data of atmospheric CO_2 concentrations.

4 DISCUSSION

Rigorous assessment of ice core CO_2 data have been used to discuss the effects of atmospheric carbon supply on the physiological responses of *N. dombeyi* since the last 15,300 yr BP (Marcott et al. 2014, Monnin et al. 2001, Monnin et al. 2004). The sensitiveness of plant species to changes in [CO_2] span on time scales of weeks to thousands of years (Beerling & Chaloner 1993a, Murray 1995). It seems likely that the effect of [CO_2] changes since late Pleistocene on the morphological and physiological stomatal characteristics of *N. dombeyi* to be operating over thousands rather over shorter periods of time, and being the magnitude of CO_2 changes a determinant factor on the long-term adaptations of this species to changes of [CO_2] (Franks et al. 2012). In the light of this consideration, it appears appropriate for *N. dombeyi* that while keeping unchanged the stomatal size, and maintaining the stomatal diffusion pathway (taken here as the width of a single guard cell), it modulates the number and length of the stomatal pore in response to [CO_2] changes. Premoli and Brewer (2007) previously reported the unchanged SS in *Nothofagus*, thus, it is likely SS could be phylogenetically conserved in this genus, in the same way as other traits that have previously been reported for *Nothofagus* (Glade-Vargas et al. 2018). The reduction in stomatal number and pore size has been proposed as a way to reduce conductance as the atmospheric CO_2 concentrations increase (Franks & Beerling 2009, Franks et al. 2012, Woodward &

Bazzaz 1988). Accordingly, both the number and *pl* variation in this study is consistent with the rise of [CO_2] since late Pleistocene.

The higher maximum stomatal conductance capacity of samples from late Pleistocene and Holocene, reflects that the dynamic stomatal behavior in these individuals should be operating in a way to improve the diffusion of CO_2 from the atmosphere to the mesophyll cells, by increasing the cross-sectional area of the diffusive pathway (Maherali et al. 2002, Parkhurst 1994) and the stomatal densities (Franks et al. 2009, Woodward & Bazzaz 1988). Thus, changes in $g_{c(max)}$ of *N. dombeyi* from late Pleistocene to current time, have been shown to be an effective and efficient way of controlling plant performance under environmental conditions of low [CO_2]. The higher $g_{c(max)}$ values in late Pleistocene samples resulted in significant c_i/c_a increases, which in turn increased the levels of $\Delta\delta^{13}C$, and collectively these responses resulted in more negative $\delta^{13}C$ values. These results support previous research in LGM studies using similar analysis in which it is demonstrate that plants were functioning with high stomatal conductance (Beerling & Woodward 1993, Beerling 1996, Beerling & Woodward 1995, Van de Water et al. 1994). Oppositely, as a result of current higher levels of CO_2 in the atmosphere, lower $g_{c(max)}$ values in the modern samples have led reduced c_i/c_a and $\Delta\delta^{13}C$ values, which ultimately resulted in less negative $\delta^{13}C$ values.

Some ecophysiological studies on plants from the LGM and Holocene conducted by Beerling and Woodward (1993), Van de Water et al. (1994), and Cowling and Sykes (1999), have attributed these responses to low rates of photosynthesis and low water use efficiency (WUE). On the other hand, an invariable c_i/c_a ratio since LGM has been

attributed to higher photosynthetic rates (Becklin et al. 2014, Gerhart & Ward 2010, Ward et al. 2005). This however is a highly unlikely scenario in view of the physiological characteristics derived from the $\delta^{13}C$ data and the percent abundances of foliar nitrogen concentrations in the leaf samples of *N. dombeyi* here analyzed. Leaf Nitrogen content and photosynthetic capacity have shown to have a positive and significant relationship (Evans 1989, Reich et al. 1998, Reich et al. 1995, Field 1983). The studies conducted by Hollinger (1989, 1996) for different *Nothofagus* species showed as well that photosynthesis increased with leaf Nitrogen content. Therefore, the lower leaf N content of leaf samples from the late Pleistocene, could had been exerting a differential influence over the amount of photosynthetic enzymes (Nijs et al. 1995, Schulze et al. 1994), that could resulted in lower carbon assimilation rates, with respect to that exerted by the high leaf N content of modern samples. Here, the scaling method for estimating maximum CO_2 assimilation rates using data of leaf nitrogen concentration and maximum stomatal conductance of Schulze et al. (1994), was used to predict the photosynthetic capacity in *N. dombeyi* samples. As expected, photosynthetic capacity positively correlated with the leaf N content (Appendix III).

The values of c_i/c_a ratio could be used as an indicator of the differences in the photosynthetic capacity of *N. dombeyi* in connection with the changes in [CO_2] since late Pleistocene. Whether it is taken as a reference to understand the regulation of water vapour loss through stomata (Prentice et al. 2014), or as a reference to understand how $g_{c(max)}$ correlates with the capacity for CO_2 fixation; i.e. a highest *ci/ca* ratio indicate that $g_{c(max)}$ is large in relation to the process of carbon fixation, which in turn is the result of a

low WUE (Farquhar et al. 1982). Also, the WUE values have been correlated to $\Delta\delta^{13}C$; i.e. Farquhar et al. (1982) have shown that those C3 plants that have the greatest WUE appears to have the lowest $\Delta\delta^{13}C$ levels. While Farquhar and Richards (1984) have found that in winter, plants tend to have highest $\Delta\delta^{13}C$ levels, possibly because the lower value of leaf-to-air vapour pressure difference caused stomatal to opening and increased c_i/c_a.

Regardless of the differential effects of $g_{c(max)}$ on c_i/c_a, $\Delta\delta^{13}C$, $\delta^{13}C$, and c_i at each epoch, it is worth mentioning that overall, this trait seems to be fundamental for the plant functioning improvements of *N. dombeyi* since late Pleistocene. A time span increases of stomatal opening during unfavorable conditions is a response previously reported for modern *Nothofagus* species by Zuniga et al. (2006), and Piper et al. (2007), as well as becoming faster to close under stress conditions to maintain or enhance the balance between carbon gain and the rate of water loss. Field and experimental studies have demonstrated that a high stomatal conductance capacity of *N. dombeyi* explained in part the high tolerance of this species to stress conditions (Sanhueza et al. 2015, Zuniga et al. 2006). Additionally, it has shown to have a high cold hardiness level which means that the lowest temperature that can be tolerated causing injury to 50% of the leaf tissues is -14.3ºC (Reyes-Díaz et al. 2005). Water lose observation in *N. dombeyi* leaves also revealed a high desiccation tolerance as the ability to survive when naturally exposed to this stress (Weinberger 1977).

Estimated CO_2 from modern samples approaches current concentrations of atmospheric CO_2 (405 ppm; Keeling & Keeling 2017). However, the model overestimated CO_2

levels for the late Pleistocene and Holocene when current *N. dombeyi*'s assimilation rate was used. Therefore, the unreliable estimations of [CO_2] from the late Pleistocene and mid-Holocene, limited the incorporation of this data into the CO_2 responses of stomata (morphological and physiological) analysis. Because the model assumed static variable inputs that are based upon modern empirical data, sensitivity analysis has been applied to investigate the degree of uncertainty of these parameters in the estimated CO_2. From all of the model inputs, the light-saturated photosynthetic rate at a known level of CO_2 (*A0*: 12 μmol m-2s-1 at 360 ppm of CO_2) and the scaling factor between maximum conductance (as calculated from stomatal geometry) to operational conductance ($g_{c(op)}$/ $g_{c(max)}$), have previously reported to affect estimated CO_2 (Maxbauer et al. 2014), so they were chosen to perform the sensitivity analysis.

If the photosynthetic rate scales proportionally with [CO_2] (Franks et al. 2013), and leaf Nitrogen content (Reich et al. 1995), the late Pleistocene and Holocene *A0* values might be lower than those from modern time. Sensitivity analysis showed that by setting a default value for *A0* as the lower empirical values obtained using drought-stressed *N. dombeyi* seedlings (0.8 μmol m-2s-1, Sanhueza et al. 2015), this parameter alone can reduce estimated CO_2 from ~700 to less than ~400 ppm (Appendix IVA). However, it is unlikely late Pleistocene or Holocene *N. dombeyi* populations were operating under such a lower *A0* scenario. First, under field conditions, the lower *A0* registered for this species was 2.4 μmol $m^{-2}s^{-1}$ (Sanhueza et al. 2015), demonstrating that *N. dombeyi* responses to a combination of natural stresses could be different to those seen under experimental individual stresses. Second, the gas exchanges measurements on single experiments could restrain a broad range of strategies in response to environmental changes.

Franks et al. (2014) assume a $g_{c(op)}/g_{c(max)}$ ratio of 0.2 based on measurements from some extant species. However, the higher SD of late Pleistocene and Holocene samples, may have increased $g_{c(max)}$ which will reduce the $g_{c(op)}/ g_{c(max)}$ ratio, causing the CO_2 estimates to go up. While in modern plants, the lower SD, reduced the $g_{c(max)}$, and raise the $g_{c(op)}/ g_{c(max)}$ ratio, which will have caused the CO_2 estimates to go down. Therefore, the $g_{c(op)}/ g_{c(max)}$ for late Pleistocene and Holocene samples should be set to higher values than those for extant species as shown in the Appendix IVB. On the other hand, from the model inputs derived from specific leaf stomatal and $\delta^{13}C$ measurements, the leaf $\delta^{13}C$ explained to a greater extent the highest values for paleo [CO_2] obtained from the fossil leaves. The more negative the $\delta^{13}C$, the higher the estimated [CO_2] (Appendix V). Nonetheless, as described in the new gas-exchanged model of paleo-atmospheric CO_2 estimations, the inputs are inter-related and feedback on one others, thus, the output that emerged from this system would require much research to obtain a comprehensive review of the ways each input and its feedback affect estimated CO_2.

5 CONCLUSION

Here it was hypothesized that the lower [CO_2] during the late Pleistocene and mid-Holocene would be exerting a selective pressure on plant populations of *N. dombeyi*, so that, individuals would have come up with adjustments on the morphological and physiological stomatal characteristics to promote plant functioning under these scenarios, and differed from those of modern population exposed to higher [CO_2]. This study showed that during the late Pleistocene and mid-Holocene plant populations of *N. dombeyi* had higher stomatal density, longer pores, higher stomatal conductance, higher c_i/c_a ratios, and higher $\Delta\delta^{13}C$. In contrast, modern population have showed a reduction in their stomatal density, pore length, stomatal conductance, c_i/c_a ratios, and $\Delta\delta^{13}C$.

By performing this comprehensive analysis of morphological and physiological characteristics, this study provides new insights on the morphological mechanisms controlling the physiological responses that have led to fast adaptation of *N. dombeyi* to short-term and extreme environmental changes from the late Pleistocene to modern days. Changes in SD and *pl* were found to be responsible for the variation in $g_{c(max)}$, which in turn was found to be related to the variation in $\Delta\delta^{13}C$, c_i/c_a, $\delta^{13}C$, and c_i suggesting that adjustments to both morphological and physiological characteristic have lead individuals to come up in this way to defeat adverse conditions, promoting plant functioning different from those of modern population exposed to higher [CO2]. Thus,

these mechanisms may have either conferred advantages to maintain populations under these conditions, or increased opportunities for new colonization, and that in turn, may help explain the rich microfossil record of this species over the last glacial-interglacial cycle. Additionally, it provides a framework to guide future research that may help elucidate the role of CO_2 in driving the evolution of future ecosystems in the southern part of South America by elucidating underlying mechanism of plant functioning strategies under changing atmospheric CO_2 concentrations.

6 REFERENCES

Ahn, J. & E. J. Brook (2014) Siple Dome ice reveals two modes of millennial CO2 change during the last ice age. *Nature Communications,* 5**,** 3723.

Ainsworth, E. A. & S. P. Long (2005) What have we learned from 15 years of free-air CO2 enrichment (FACE)? A meta-analytic review of the responses of photosynthesis, canopy properties and plant production to rising CO2. *New Phytologist,* 165**,** 351-372.

Alberdi, M. (1987) Ecofisiología de especies Chilenas del género Nothofagus. *Bosque,* 8**,** 77 - 84.

Becklin, K. M., J. S. Medeiros, K. R. Sale & J. K. Ward (2014) Evolutionary history underlies plant physiological responses to global change since the last glacial maximum. *Ecology letters,* 17**,** 691-699.

Beerling, D. & F. Woodward (1993) Ecophysiological responses of plants to global environmental change since the Last Glacial Maximum. *New Phytologist,* 125**,** 641-648.

Beerling, D. J. (1996) 13C discrimination by fossil leaves during the late-glacial climate oscillation 12-10 ka BP: measurements and physiological controls. *Oecologia,* 108**,** 29-37.

Beerling, D. J. & W. G. Chaloner (1993a) Evolutionary responses of stomatal density to global CO2 change. *Biological Journal of the Linnean Society,* 48**,** 343-353.

Beerling, D. J. & W. G. Chaloner (1993b) The impact of atmospheric CO2 and temperature changes on stomatal density: Observation from Quercus robur Lammas leaves. *Annals of Botany,* 71**,** 231-235.

Beerling, D. t. & F. Woodward (1995) Leaf stable carbon isotope composition records increased water-use efficiency of C 3 plants in response to atmospheric CO 2 enrichment. *Functional Ecology***,** 394-401.

Bennett, K. D., S. G. Haberle & S. H. Lumley (2000) The last Glacial-Holocene transition in southern Chile. *Science,* 290**,** 325-328.

Cernusak, L. A., K. Winter, J. W. Dalling, J. A. Holtum, C. Jaramillo, C. Körner, A. D. Leakey, R. J. Norby, B. Poulter & B. L. Turner (2013) Tropical forest responses

to increasing atmospheric CO2: current knowledge and opportunities for future research. *Functional Plant Biology,* 40**,** 531-551.

Cowling, S. A. & M. T. Sykes (1999) Physiological significance of low atmospheric CO2 for plant–climate interactions. *Quaternary Research,* 52**,** 237-242.

Curtis, P. S. & X. Wang (1998) A meta-analysis of elevated CO2 effects on woody plant mass, form, and physiology. *Oecologia,* 113**,** 299-313.

Dippery, J. K., D. T. Tissue, R. B. Thomas & B. R. Strain (1995) Effects of low and elevated CO2 on C3 and C4 annuals. *Oecologia,* 101**,** 13-20.

Eggleston, S., J. Schmitt, B. Bereiter, R. Schneider & H. Fischer (2016) Evolution of the stable carbon isotope composition of atmospheric CO2 over the last glacial cycle. *Paleoceanography,* 31**,** 434-452.

Evans, J. R. (1989) Photosynthesis and nitrogen relationships in leaves of C 3 plants. *Oecologia,* 78**,** 9-19.

Farquhar, G. & R. Richards (1984) Isotopic composition of plant carbon correlates with water-use efficiency of wheat genotypes. *Functional Plant Biology,* 11**,** 539-552.

Farquhar, G. D., J. R. Ehleringer & K. T. Hubick (1989) Carbon isotope discrimination and photosynthesis. *Annual Review of Plant Physiology and Plant Molecular Biology,* 40**,** 503-537.

Farquhar, G. D., M. H. O'Leary & J. A. Berry (1982) On the relationship between carbon isotope discrimination and the intercellular carbon dioxide concentration in leaves. *Functional Plant Biology,* 9**,** 121-137.

Farquhar, G. D. & T. D. Sharkey (1982) Stomatal conductance and photosynthesis. *Annual Review of Plant Physiology,* 33**,** 317-345.

Field, C. (1983) Allocating leaf nitrogen for the maximization of carbon gain: Leaf age as a control on the allocation program. *Oecologia,* 56**,** 341-347.

Fox, J. & S. Weisberg (2011) An {R} Companion to Applied Regression. *Thousand Oaks CA: Sage.,* Second Edition.

Franks, P. J., M. A. Adams, J. S. Amthor, M. M. Barbour, J. A. Berry, D. S. Ellsworth, G. D. Farquhar, O. Ghannoum, J. Lloyd, N. McDowell, R. J. Norby, D. T. Tissue & S. Caemmerer (2013) Sensitivity of plants to changing atmospheric CO2 concentration: from the geological past to the next century. *New Phytologist,* 197**,** 1077-1094.

Franks, P. J. & D. J. Beerling (2009) Maximum leaf conductance driven by CO2 effects on stomatal size and density over geologic time. *Proceedings of the National Academy of Sciences,* 106**,** 10343-10347.

Franks, P. J., P. L. Drake & D. J. Beerling (2009) Plasticity in maximum stomatal conductance constrained by negative correlation between stomatal size and density: an analysis using Eucalyptus globulus. *Plant, cell & environment,* 32**,** 1737-1748.

Franks, P. J., I. J. Leitch, E. M. Ruszala, A. M. Hetherington & D. J. Beerling (2012) Physiological framework for adaptation of stomata to CO2 from glacial to future concentrations. *Philosophical Transactions of the Royal Society B: Biological Sciences,* 367**,** 537-546.

Franks, P. J., D. L. Royer, D. J. Beerling, P. K. Van de Water, D. J. Cantrill, M. M. Barbour & J. A. Berry (2014) New constraints on atmospheric CO2 concentration for the Phanerozoic. *Geophysical Research Letters,* 41**,** 4685-4694.

Gerhart, L. M. & J. K. Ward (2010) Plant responses to low [CO2] of the past. *New Phytologist,* 188**,** 674-695.

Glade-Vargas, N., L. F. Hinojosa & M. Leppe (2018) Evolution of climatic related leaf traits in the family Nothofagaceae. *Frontiers in plant science,* 9**,** 1073-1073.

Heusser, C. J. (1981) Palynology of the last interglacial-glacial cycle in midlatitudes of Southern Chile. *Quaternary Research,* 16**,** 293-321.

Heusser, C. J., L. E. Heusser & T. V. Lowell (1999) Paleoecology of the southern chilean lake district-isla grande de chiloé during middle–late llanquihue glaciation and deglaciation. *Geografiska Annaler: Series A, Physical Geography,* 81**,** 231-284.

Hollinger, D. (1989) Canopy organization and foliage photosynthetic capacity in a broad-leaved evergreen montane forest. *Functional Ecology***,** 53-62.

--- (1996) Optimality and nitrogen allocation in a tree canopy. *Tree Physiology,* 16**,** 627-634.

Jouzel, J., N. I. Barkov, J. M. Barnola, M. Bender, J. Chappellaz, C. Genthon, V. M. Kotlyakov, V. Lipenkov, C. Lorius, J. R. Petit, D. Raynaud, G. Raisbeck, C. Ritz, T. Sowers, M. Stievenard, F. Yiou & P. Yiou (1993) Extending the Vostok ice-core record of palaeoclimate to the penultimate glacial period. *Nature,* 364**,** 407.

Jouzel, J., C. Lorius, J. R. Petit, C. Genthon, N. I. Barkov, V. M. Kotlyakov & V. M. Petrov (1987) Vostok ice core: a continuous isotope temperature record over the last climatic cycle (160,000 years). *Nature,* 329**,** 403.

Jouzel, J., C. Waelbroeck, B. Malaize, M. Bender, J. R. Petit, M. Stievenard, N. I. Barkov, J. M. Barnola, T. King, V. M. Kotlyakov, V. Lipenkov, C. Lorius, D. Raynaud, C. Ritz & T. Sowers (1996) Climatic interpretation of the recently extended Vostok ice records. *Climate Dynamics,* 12**,** 513-521.

Keeling, C. D., S. C. Piper, R. B. Bacastow, M. Wahlen, T. P. Whorf, M. Heimann & H. A. Meijer (2001) Exchanges of atmospheric CO2 and 13CO2 with the terrestrial biosphere and oceans from 1978 to 2000. I. Global aspects.

Keeling, R. F. & C. D. Keeling (2017) Atmospheric monthly in situ CO2 data - Mauna Loa Observatory, Hawaii. *In Scripps CO2 Program Data. UC San Diego Library Digital Collections*.

Lambers, H., F. S. Chapin & T. L. Pons. 1998. Photosynthesis, respiration, and long-distance transport. In *Plant Physiological Ecology,* eds. H. Lambers, F. S. Chapin & T. L. Pons, 10-153. New York, NY: Springer New York.

Lloyd, J. & G. D. Farquhar (2008) Effects of rising temperatures and [CO2] on the physiology of tropical forest trees. *Philosophical Transactions of the Royal Society of London B: Biological Sciences,* 363**,** 1811-1817.

Lourantou, A., J. V. Lavrič, P. Köhler, J.-M. Barnola, D. Paillard, E. Michel, D. Raynaud & J. Chappellaz (2010) Constraint of the CO2 rise by new atmospheric carbon isotopic measurements during the last deglaciation. *Global Biogeochemical Cycles,* 24.

Lusk, C. H., I. Wright & P. B. Reich (2003) Photosynthetic differences contribute to competitive advantage of evergreen angiosperm trees over evergreen conifers in productive habitats. *New Phytologist,* 160**,** 329-336.

MacFarling Meure, C., D. Etheridge, C. Trudinger, P. Steele, R. Langenfelds, T. Van Ommen, A. Smith & J. Elkins (2006) Law Dome CO2, CH4 and N2O ice core records extended to 2000 years BP. *Geophysical Research Letters,* 33.

Maherali, H., C. D. Reid, H. W. Polley, H. B. Johnson & R. B. Jackson (2002) Stomatal acclimation over a subambient to elevated CO2 gradient in a C3/C4 grassland. *Plant, Cell & Environment,* 25**,** 557-566.

Marcott, S. A., T. K. Bauska, C. Buizert, E. J. Steig, J. L. Rosen, K. M. Cuffey, T. Fudge, J. P. Severinghaus, J. Ahn & M. L. Kalk (2014) Centennial-scale changes in the global carbon cycle during the last deglaciation. *Nature,* 514**,** 616.

Markgraf, V. (1991) Younger Dryas in southern South America? *Boreas,* 20**,** 63-69.

Markgraf, V., R. S. Webb, K. H. Anderson & L. Anderson (2002) Modern pollen/climate calibration for southern South America. *Palaeogeography, Palaeoclimatology, Palaeoecology,* 181**,** 375-397.

Maxbauer, D. P., D. L. Royer & B. A. LePage (2014) High Arctic forests during the middle Eocene supported by moderate levels of atmospheric CO2. *Geology,* 42**,** 1027-1030.

McElwain, J. C. & W. G. Chaloner (1995) Stomatal density and index of fossil plants track atmospheric carbon dioxide in the Palaeozoic. *Annals of Botany,* 76**,** 389-395.

Meza-Basso, L., P. Guarda, D. Rios & M. Alberdi (1986) Changes in free amino acid content and frost resistance in Nothofagus dombeyi leaves. *Phytochemistry,* 25**,** 1843-1846.

Monnin, E., A. Indermühle, A. Dällenbach, J. Flückiger, B. Stauffer, T. F. Stocker, D. Raynaud & J.-M. Barnola (2001) Atmospheric CO2 Concentrations over the Last Glacial Termination. *Science,* 291**,** 112-114.

Monnin, E., E. J. Steig, U. Siegenthaler, K. Kawamura, J. Schwander, B. Stauffer, T. F. Stocker, D. L. Morse, J.-M. Barnola, B. Bellier, D. Raynaud & H. Fischer (2004) Evidence for substantial accumulation rate variability in Antarctica during the Holocene, through synchronization of CO2 in the Taylor Dome, Dome C and DML ice cores. *Earth and Planetary Science Letters,* 224**,** 45-54.

Moreno, P. I. & A. L. León (2003) Abrupt vegetation changes during the last glacial to Holocene transition in mid-latitude South America. *Journal of Quaternary Science,* 18**,** 787-800.

Moreno, P. I., T. V. Lowell, G. L. Jacobson Jr & G. H. Denton (1999) Abrupt vegetation and climate changes during the last glacial maximumand last termination in the chilean lake district: a case study from canal de la puntilla (41° s). *Geografiska Annaler: Series A, Physical Geography,* 81**,** 285-311.

Moreno, P. I., J. Videla, B. Valero-Garcés, B. V. Alloway & L. E. Heusser (2018) A continuous record of vegetation, fire-regime and climatic changes in northwestern Patagonia spanning the last 25,000 years. *Quaternary Science Reviews,* 198**,** 15-36.

Murray, D. R. (1995) Plant responses to carbon dioxide. *American Journal of Botany,* 82**,** 690-697.

Nijs, I., T. Behaeghe & I. Impens (1995) Leaf nitrogen content as a predictor of photosynthetic capacity in ambient and global change conditions. *Journal of Biogeography*, 177-183.

Pagani, M., Z. Liu, J. LaRiviere & A. C. Ravelo (2009) High Earth-system climate sensitivity determined from Pliocene carbon dioxide concentrations. *Nature Geoscience,* 3, 27.

Parkhurst, D. F. (1994) Diffusion of CO2 and other gases inside leaves. *New Phytologist,* 126, 449-479.

Pedro, J. B., H. C. Bostock, C. M. Bitz, F. He, M. J. Vandergoes, E. J. Steig, B. M. Chase, C. E. Krause, S. O. Rasmussen & B. R. Markle (2016) The spatial extent and dynamics of the Antarctic Cold Reversal. *Nature Geoscience,* 9, 51.

Pépin, L., D. Raynaud, J.-M. Barnola & M. F. Loutre (2001) Hemispheric roles of climate forcings during glacial-interglacial transitions as deduced from the Vostok record and LLN-2D model experiments. *Journal of Geophysical Research: Atmospheres,* 106, 31885-31892.

Petit, J., D. Raynaud, C. Lorius, J. Jouzel, G. Delaygue, N. Barkov & V. Kotlyakov (2000) Historical isotopic temperature record from the Vostok ice core. *Trends: A Compendium of Data on Global Change*.

Petit, J. R., J. Jouzel, D. Raynaud, N. I. Barkov, J. M. Barnola, I. Basile, M. Bender, J. Chappellaz, M. Davis, G. Delaygue, M. Delmotte, V. M. Kotlyakov, M. Legrand, V. Y. Lipenkov, C. Lorius, L. PÉpin, C. Ritz, E. Saltzman & M. Stievenard (1999) Climate and atmospheric history of the past 420,000 years from the Vostok ice core, Antarctica. *Nature,* 399, 429.

Piper, F. I., L. J. Corcuera, M. Alberdi & C. Lusk (2007) Differential photosynthetic and survival responses to soil drought in two evergreen Nothofagus species. *Annals of Forest Science,* 64, 447-452.

Premoli, A. C. & C. A. Brewer (2007) Environmental v. genetically driven variation in ecophysiological traits of Nothofagus pumilio from contrasting elevations. *Australian Journal of Botany,* 55, 585-591.

Prentice, I. C., N. Dong, S. M. Gleason, V. Maire & I. J. Wright (2014) Balancing the costs of carbon gain and water transport: testing a new theoretical framework for plant functional ecology. *Ecology Letters,* 17, 82-91.

Raynaud, D., J.-M. Barnola, R. Souchez, R. Lorrain, J.-R. Petit, P. Duval & V. Y. Lipenkov (2005) The record for marine isotopic stage 11. *Nature,* 436, 39.

Reich, P., D. Ellsworth & M. Walters (1998) Leaf structure (specific leaf area) modulates photosynthesis–nitrogen relations: evidence from within and across species and functional groups. *Functional Ecology,* 12**,** 948-958.

Reich, P., M. Walters, B. Kloeppel & D. Ellsworth (1995) Different photosynthesis-nitrogen relations in deciduous hardwood and evergreen coniferous tree species. *Oecologia,* 104**,** 24-30.

Reyes-Díaz, M., M. Alberdi, F. Piper, L. A. Bravo & L. J. Corcuera (2005) Low temperature responses of Nothofagus dombeyi and Nothofagus nitida, two evergreen species from south central Chile. *Tree physiology,* 25**,** 1389-1398.

Royer, D. (2001) Stomatal density and stomatal index as indicators of paleoatmospheric CO2 concentration. *Review of Palaeobotany and Palynology,* 114**,** 1-28.

Sage, R. F. & J. R. Coleman (2001) Effects of low atmospheric CO2 on plants: more than a thing of the past. *Trends in plant science,* 6**,** 18-24.

Sanhueza, C., L. Bascunan-Godoy, M. H. Turnbull & L. J. Corcuera (2015) Response of photosynthesis and respiration to temperature under water deficit in two evergreen Nothofagus species. *Plant Species Biology,* 30**,** 163-175.

Schmitt, J., R. Schneider, J. Elsig, D. Leuenberger, A. Lourantou, J. Chappellaz, P. Köhler, F. Joos, T. F. Stocker, M. Leuenberger & H. Fischer (2012) Carbon isotope constraints on the deglacial CO2 rise from ice cores. *Science,* 336**,** 711-714.

Schulze, E.-D., F. M. Kelliher, C. Korner, J. Lloyd & R. Leuning (1994) Relationships Among Maximum Stomatal Conductance, Ecosystem Surface Conductance, Carbon Assimilation Rate, and Plant Nitrogen Nutrition: A Global Ecology Scaling Exercise. *Annual Review of Ecology and Systematics,* 25**,** 629-660.

Seki, O., G. L. Foster, D. N. Schmidt, A. Mackensen, K. Kawamura & R. D. Pancost (2010) Alkenone and boron-based Pliocene pCO2 records. *Earth and Planetary Science Letters,* 292**,** 201-211.

Street-Perrott, F. A., Y. Huang, R. A. Perrott, G. Eglinton, P. Barker, L. B. Khelifa, D. D. Harkness & D. O. Olago (1997) Impact of lower atmospheric carbon dioxide on tropical mountain ecosystems. *Science,* 278**,** 1422-1426.

Stuiver, M. & P. J. Reimer (1993) Extended 14 C data base and revised CALIB 3.0 14 C age calibration program. *Radiocarbon,* 35**,** 215-230.

Van de Water, P. K., S. W. Leavitt & J. Betancourt (1994) Trends in stomatal density and 13C/12C ratios of Pinus flexilis needles during last glacial-interglacial cycle. *Science,* 264**,** 239-243.

Veblen, T. T., R. S. Hill & J. Read. 1996. *The ecology and biogeography of Nothofagus forests*. Yale University Press.

Villagrán, C., A. León & F. A. Roig (2004) Paleodistribución del alerce y ciprés de las Guaitecas durante períodos interestadiales de la Glaciación Llanquihue: provincias de Llanquihue y Chiloé, Región de Los Lagos, Chile. *Revista geológica de Chile,* 31**,** 133-151.

Villagrán, C. M. 1995. Quaternary History of the Mediterranean Vegetation of Chile. In *Ecology and Biogeography of Mediterranean Ecosystems in Chile, California, and Australia,* eds. M. T. K. Arroyo, P. H. Zedler & M. D. Fox, 3-20. New York, NY: Springer New York.

Von Caemmerer, S. 2000. *Biochemical models of leaf photosynthesis*. Csiro publishing.

Ward, J. K., J. M. Harris, T. E. Cerling, A. Wiedenhoeft, M. J. Lott, M.-D. Dearing, J. B. Coltrain & J. R. Ehleringer (2005) Carbon starvation in glacial trees recovered from the La Brea tar pits, southern California. *Proceedings of the National Academy of Sciences,* 102**,** 690-694.

Weinberger, P. (1977) The regeneration of the Araucano - Patagonic Nothofagus species in relation to microclimatic conditions. *Tuatara,* 22**,** 245 - 266.

Wickham, H., R. Francois, L. Henry & K. Müller (2017) dplyr: A Grammar of Data Manipulation. . *R package version 0.7.4.*

Winter, K., J. Aranda, M. Garcia, A. Virgo & S. R. Paton (2001) Effect of elevated CO2 and soil fertilization on whole-plant growth and water use in seedlings of a tropical pioneer tree, Ficus insipida Willd. *Flora,* 196**,** 458-464.

Woodward, F. I. (1987) Stomatal numbers are sensitive to increases in CO2 from pre-industrial levels. *Nature,* 327**,** 617.

Woodward, F. I. & F. A. Bazzaz (1988) The responses of stomatal density to CO2 partial pressure. *Journal of Experimental Botany,* 39**,** 1771-1781.

Zegers, C. D. (1989) Antecedentes básicos para la silvicultura del tipo forestal siempreverde. *Bosque (Valdivia),* 10.

Zuniga, R., M. Alberdi, M. Reyes-Diaz, E. Olivares, S. Hess, L. A. Bravo & L. J. Corcuera (2006) Seasonal changes in the photosynthetic performance of two evergreen Nothofagus species in south central Chile. *Revista Chilena de Historia Natural,* 79.

APPENDIX

Appendix I. Leaf assemblage across the late Pleistocene and Holocene (15,400 – 4,900 yr. BP) in the Río Caunahué outcrop, Región de los Lagos, Chile (Hinojosa, L.F. unpublished data).

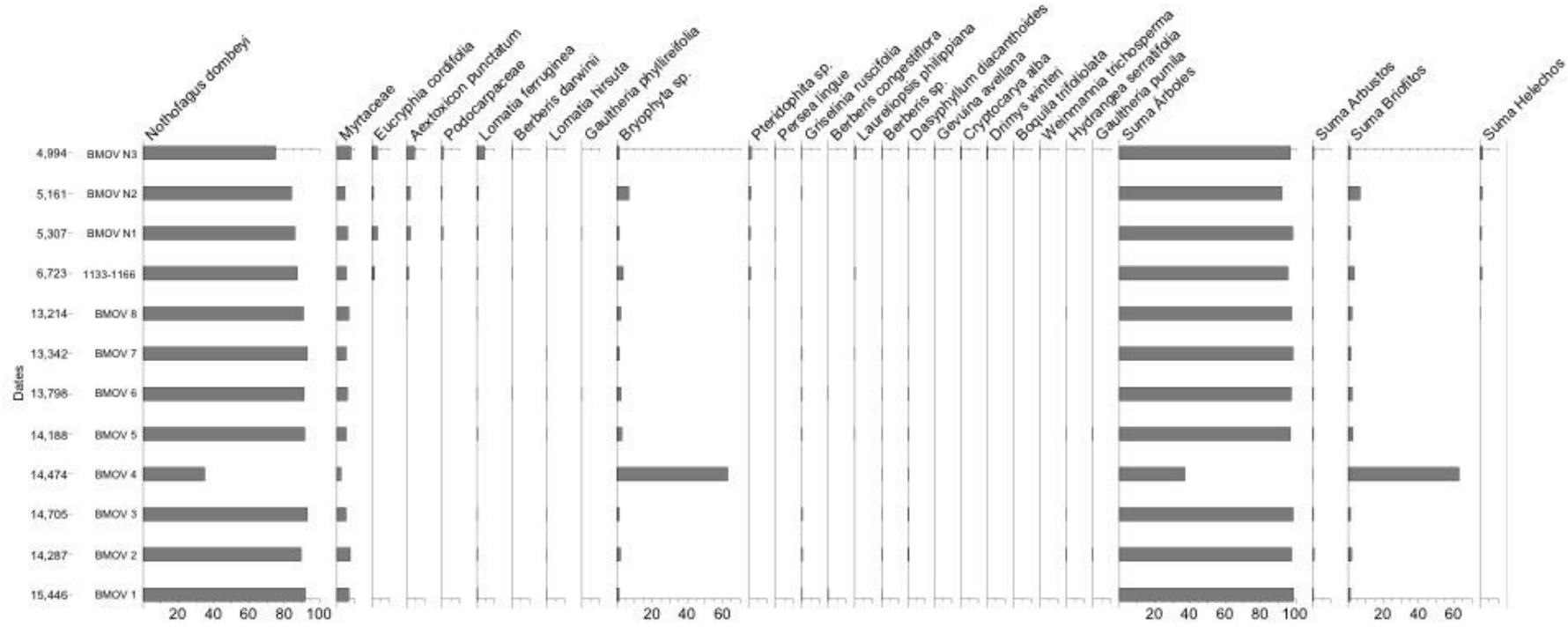

Appendix II. Morphological data: stomatal density (SD; number of stomata per mm^2), pore length (*pl*; µm), guard cell width (*gcw*; µm), and stomatal size (SS; µm). Physiological data: anatomical maximum stomatal conductance ($g_{c(max)}$; mol m^{-2} s^{-1}), stable carbon isotope ratio ($\delta^{13}C$; ‰), carbon isotope discrimination ($\Delta\delta^{13}C$; ‰), the inter-cellular to atmospheric CO_2 ratio (c_i/c_a)), and the inter-cellular CO_2 concentration (c_i; ppm) of different sets of fossil and modern leaf samples of *Nothofagus dombeyi*.

Epoch	Age (years BP)	Sample ID	SD	*pl*	*gcw*	SS	$g_{c(max)}$	$\delta^{13}C$	$\Delta\delta^{13}C$	c_i/c_a	c_i	Leaf %N
Late Pleistocene	15336	A1	556	9.0	10.1	772	1.12	-30.94	25.22	0.81	187	0.63
Late Pleistocene	15336	A2	472	10.1	9.7	720	1.24	-29.17	23.35	0.74	170	0.81
Late Pleistocene	15336	A3	479	10.0	9.4	669	1.36	-27.48	21.57	0.67	154	0.81
Late Pleistocene	15336	A4	413	10.0	10.0	752	1.03	-31.56	25.88	0.84	193	0.7
Late Pleistocene	15336	A5	397	9.3	9.7	826	0.88	-29.54	23.75	0.76	174	0.64
Late Pleistocene	15336	A6	469	9.4	9.3	673	1.09	-29.08	23.25	0.74	169	0.4
Late Pleistocene	15336	A7	389	10.8	9.7	819	1.10	-28.22	22.35	0.70	161	0.59
Late Pleistocene	15336	A8	553	10.1	9.6	725	1.43	-28.76	22.92	0.72	166	0.63
Late Pleistocene	15336	A9	445	9.1	10.0	801	1.04	-28.41	22.55	0.71	163	0.28
Late Pleistocene	15336	A10	546	9.2	9.5	678	1.27	-27.07	21.15	0.65	150	0.6
Late Pleistocene	14660	B1	365	9.5	10.0	868	0.88	-28.21	22.34	0.70	161	0.96
Late Pleistocene	14660	B2	462	9.4	9.7	804	1.08	-30.31	24.55	0.79	181	0.48
Late Pleistocene	14660	B3	441	9.1	9.4	759	1.02	-27.89	22.01	0.69	158	0.78
Late Pleistocene	14660	B4	421	9.9	9.4	798	1.17	-29.20	23.38	0.74	171	0.37
Late Pleistocene	14660	B5	387	9.8	9.4	952	1.04	-30.89	25.17	0.81	187	0.48
Late Pleistocene	14660	B6	440	8.7	10.0	680	0.91	-28.10	22.22	0.70	160	0.35

Late Pleistocene	14660	B7	490	9.7	9.4	670	1.18	-29.93	24.16	0.77	178	0.39
Late Pleistocene	14660	B8	427	10.1	10.1	708	1.08	-29.23	23.41	0.74	171	0.3
Late Pleistocene	14660	B9	561	10.3	9.9	583	1.56	-30.38	24.63	0.79	182	0.82
Late Pleistocene	14660	B10	387	10.6	9.5	806	1.09	-30.04	24.27	0.78	178	0.59
Late Pleistocene	14837	C1	349	10.7	10.0	730	0.96	-30.14	24.37	0.78	179	0.94
Late Pleistocene	14837	C2	432	10.0	9.8	708	1.13	-30.90	25.17	0.81	187	0.63
Late Pleistocene	14837	C3	425	9.9	9.8	771	1.13	-28.82	22.98	0.73	167	0.34
Late Pleistocene	14837	C4	437	9.1	8.8	590	1.02	-30.36	24.61	0.79	182	0.87
Late Pleistocene	14837	C5	425	9.6	8.8	740	1.13	-29.98	24.21	0.77	178	0.7
Late Pleistocene	14837	C6	493	11.5	10.3	817	1.59	-31.03	25.32	0.82	188	0.37
Late Pleistocene	14837	C7	350	10.1	9.8	833	0.91	-29.28	23.47	0.74	171	0.42
Late Pleistocene	14837	C8	366	10.4	9.3	883	1.05	-30.55	24.80	0.80	183	0.44
Late Pleistocene	14837	C9	530	9.5	9.2	673	1.34	-29.28	23.47	0.74	171	0.98
Late Pleistocene	14837	C10	467	9.5	9.0	687	1.16	-29.42	23.62	0.75	173	0.68
Late Pleistocene	14505	D1	359	9.3	8.8	697	0.88	-28.02	22.14	0.69	159	0.46
Late Pleistocene	14505	D2	351	9.8	9.4	742	0.84	-31.20	25.49	0.82	190	0.47
Late Pleistocene	14505	D3	427	10.5	9.9	795	1.22	-29.43	23.62	0.75	173	0.23
Late Pleistocene	14505	D4	372	9.7	9.6	675	0.92	-27.32	21.41	0.66	153	0.64
Late Pleistocene	14505	D5	372	10.5	9.3	854	1.14	-28.98	23.15	0.73	168	0.39
Late Pleistocene	14505	D6	529	9.0	9.4	655	1.18	-29.50	23.70	0.75	173	0.37
Late Pleistocene	14505	D7	515	9.5	10.1	679	1.20	-29.58	23.78	0.76	174	0.63
Late Pleistocene	14505	D8	356	10.5	9.4	745	1.05	-31.01	25.30	0.82	188	0.37
Late Pleistocene	14505	D9	354	9.8	9.6	793	0.87	-29.17	23.35	0.74	170	0.68
Late Pleistocene	14505	D10	367	9.6	9.9	689	0.89	-29.40	23.59	0.75	172	0.67
Late Pleistocene	14188	E1	417	8.8	9.1	767	0.98	-29.61	23.81	0.76	174	0.3

Late Pleistocene	14188	E2	359	9.0	9.2	679	0.81	-29.77	23.99	0.77	176	0.46
Late Pleistocene	14188	E3	420	9.4	9.2	842	0.97	-29.81	24.03	0.77	176	0.76
Late Pleistocene	14188	E4	406	10.0	9.7	845	1.11	-31.25	25.54	0.83	190	0.2
Late Pleistocene	14188	E5	420	9.4	9.3	699	0.98	-28.75	22.91	0.72	166	0.28
Late Pleistocene	14188	E6	459	8.6	9.3	692	1.03	-30.26	24.50	0.79	181	0.58
Late Pleistocene	14188	E7	383	9.9	9.7	739	1.04	-29.77	23.98	0.77	176	0.59
Late Pleistocene	14188	E8	455	10.7	9.0	718	1.39	-29.93	24.15	0.77	177	0.11
Late Pleistocene	14188	E9	406	9.5	9.6	780	0.97	-30.97	25.25	0.81	187	0.12
Late Pleistocene	14188	E10	482	10.1	9.1	759	1.32	-29.98	24.20	0.77	178	0.35
Late Pleistocene	13799	F1	378	11.3	10.5	716	1.14	-30.19	24.43	0.78	180	0.01
Late Pleistocene	13799	F2	388	9.6	9.5	739	0.91	-29.13	23.31	0.74	170	0.55
Late Pleistocene	13799	F3	366	9.0	9.2	835	0.90	-28.33	22.46	0.71	162	0.46
Late Pleistocene	13799	F4	427	8.6	9.5	748	0.89	-28.70	22.85	0.72	166	0.32
Late Pleistocene	13799	F5	386	10.1	9.2	793	1.10	-28.84	23.01	0.73	167	0.61
Late Pleistocene	13799	F6	379	10.9	10.7	932	1.09	-28.90	23.06	0.73	168	0.9
Late Pleistocene	13799	F7	452	9.0	9.3	662	1.00	-27.72	21.83	0.68	157	0.65
Late Pleistocene	13799	F8	611	8.7	8.7	650	1.31	-29.54	23.75	0.76	174	0.89
Late Pleistocene	13799	F9	505	9.4	9.3	678	1.18	-30.51	24.76	0.80	183	1.15
Late Pleistocene	13799	F10	524	10.0	8.9	718	1.43	-27.26	21.34	0.66	152	0.47
Late Pleistocene	13333	G1	487	10.6	9.6	711	1.41	-30.45	24.70	0.79	182	0.44
Late Pleistocene	13333	G2	614	9.0	8.5	604	1.45	-29.90	24.13	0.77	177	0.36
Late Pleistocene	13333	G3	381	9.1	8.8	869	0.92	-28.86	23.03	0.73	167	0.54
Late Pleistocene	13333	G4	411	10.1	9.1	905	1.12	-30.03	24.26	0.78	178	0.55
Late Pleistocene	13333	G5	361	9.9	9.1	797	0.96	-28.81	22.97	0.73	167	0.52
Late Pleistocene	13333	G6	352	9.9	10.1	844	0.91	-30.27	24.51	0.79	181	0.58

Late Pleistocene	13333	G7	500	8.9	8.7	736	1.17	-30.60	24.86	0.80	184	0.27
Late Pleistocene	13333	G8	388	9.0	9.5	736	0.89	-30.16	24.40	0.78	180	0.88
Late Pleistocene	13333	G9	410	10.2	8.6	777	1.18	-29.98	24.21	0.77	178	0.57
Late Pleistocene	13333	G10	421	9.7	9.0	707	1.09	-30.69	24.95	0.80	185	0.45
Late Pleistocene	13211	H1	457	9.7	8.8	677	1.24	-27.91	22.03	0.69	158	0.48
Late Pleistocene	13211	H2	419	9.4	8.8	782	1.07	-28.75	22.91	0.72	166	0.55
Late Pleistocene	13211	H3	468	9.7	9.8	712	1.20	-30.29	24.53	0.79	181	0.49
Late Pleistocene	13211	H4	488	8.5	8.8	580	1.06	-27.31	21.39	0.66	153	0.45
Late Pleistocene	13211	H5	530	10.2	9.9	600	1.40	-28.96	23.13	0.73	168	0.65
Late Pleistocene	13211	H6	431	9.3	9.3	699	1.08	-30.71	24.97	0.80	185	0.87
Late Pleistocene	13211	H7	548	8.8	9.3	592	1.18	-29.63	23.84	0.76	175	0.61
Late Pleistocene	13211	H8	421	9.1	10.0	842	0.93	-27.94	22.05	0.69	159	0.11
Late Pleistocene	13211	H9	430	8.5	9.0	684	0.91	-27.84	21.95	0.69	158	0.39
Late Pleistocene	13211	H10	376	10.5	9.6	784	1.08	-29.80	24.01	0.77	176	0.83
Holocene	5307	I1	461	9.1	9.1	669	1.09	-28.05	22.17	0.69	187	0.49
Holocene	5307	I2	416	9.6	9.9	763	1.06	-27.88	21.99	0.69	186	1.05
Holocene	5307	I3	424	9.0	9.3	699	1.00	-28.97	23.14	0.73	198	0.82
Holocene	5307	I4	443	9.4	9.9	846	1.09	-27.32	21.41	0.66	179	0.66
Holocene	5307	I5	394	9.0	9.7	865	0.88	-29.54	23.74	0.76	204	1.11
Holocene	5307	I6	433	9.5	9.9	662	1.06	-28.86	23.02	0.73	196	1.62
Holocene	5307	I7	333	10.3	9.8	875	0.97	-28.47	22.62	0.71	192	0.66
Holocene	5307	I8	415	9.4	9.1	609	1.05	-28.15	22.27	0.70	189	0.56
Holocene	5307	I9	353	9.3	9.7	741	0.79	-28.35	22.49	0.71	191	0.4
Holocene	5307	I10	523	9.1	9.7	675	1.13	-28.62	22.78	0.72	194	0.94
Holocene	5161	J1	594	9.1	9.3	624	1.44	-28.32	22.45	0.71	190	1.12

Holocene	5161	J2	523	9.7	10.0	718	1.23	-27.96	22.07	0.69	186	1.07
Holocene	5161	J3	430	9.1	9.6	793	0.98	-30.16	24.39	0.78	211	0.97
Holocene	5161	J4	487	8.2	9.2	647	0.97	-28.86	23.02	0.73	196	0.15
Holocene	5161	J5	490	9.5	9.3	766	1.25	-29.25	23.44	0.74	201	0.99
Holocene	5161	J6	327	9.2	9.2	708	0.77	-29.73	23.94	0.76	206	1.04
Holocene	5161	J7	383	10.6	9.7	796	1.13	-27.79	21.89	0.68	185	0.39
Holocene	5161	J8	494	9.2	9.5	697	1.09	-25.65	19.65	0.60	161	0.4
Holocene	5161	J9	552	8.5	9.2	603	1.24	-26.87	20.93	0.65	174	0.76
Holocene	5161	J10	367	8.6	9.1	650	0.75	-30.12	24.35	0.78	210	0.62
Holocene	4973	K1	329	9.9	9.4	689	0.84	-29.51	23.71	0.75	204	0.97
Holocene	4973	K2	589	9.2	9.6	680	1.36	-27.24	21.32	0.66	178	1.01
Holocene	4973	K3	345	9.6	10.3	793	0.91	-28.30	22.44	0.70	190	1.06
Holocene	4973	K4	412	8.9	9.3	773	0.91	-29.24	23.43	0.74	201	0.89
Holocene	4973	K5	344	8.5	8.8	623	0.75	-28.78	22.94	0.72	196	1.22
Holocene	4973	K6	412	9.4	9.4	735	1.02	-30.25	24.49	0.78	212	0.71
Holocene	4973	K7	386	9.4	9.6	696	0.96	-29.03	23.20	0.73	198	0.15
Holocene	4973	K8	429	9.7	9.2	655	1.07	-29.16	23.35	0.74	200	0.5
Holocene	4973	K9	435	9.3	9.7	680	1.01	-28.55	22.69	0.71	193	0.71
Holocene	4973	K10	427	9.0	9.7	687	0.95	-30.66	24.93	0.80	216	0.69
Holocene	6723	L1	398	10.1	9.7	791	1.05	-27.57	21.67	0.67	182	0.13
Holocene	6723	L2	435	8.5	9.9	727	0.87	-27.96	22.07	0.69	186	0.87
Holocene	6723	L3	286	9.1	9.8	885	0.66	-27.11	21.19	0.66	177	0.75
Holocene	6723	L4	594	8.7	9.0	606	1.36	-26.47	20.52	0.63	170	0.91
Holocene	6723	L5	509	9.1	9.4	661	1.19	-28.74	22.90	0.72	195	0.76
Holocene	6723	L6	455	10.4	10.2	804	1.31	-28.31	22.45	0.71	190	0.94

Holocene	6723	L7	443	8.7	9.4	611	0.97	-28.91	23.08	0.73	197	0.42
Holocene	6723	L8	431	8.6	9.6	654	0.96	-30.47	24.72	0.79	214	0.84
Holocene	6723	L9	426	9.4	10.4	830	0.98	-28.66	22.81	0.72	194	0.48
Holocene	6723	L10	453	8.5	9.6	697	0.91	-28.75	22.91	0.72	195	0.49
Modern	0	Cau 1	414	8.1	9.4	724	0.82	-30.00	22.16	0.69	250	0.09
Modern	0	Cau 2	387	7.9	8.8	791	0.82	-31.28	23.52	0.75	269	0.93
Modern	0	Cau 3	371	8.6	9.3	737	0.76	-31.41	23.66	0.75	271	0.67
Modern	0	Cau 4	397	7.8	8.4	661	0.73	-31.06	23.28	0.74	266	0.55
Modern	0	Cau 5	420	7.9	9.3	696	0.74	-30.38	22.57	0.71	255	0.49
Modern	0	Cau 6	349	8.9	9.9	753	0.73	-27.49	19.52	0.59	213	0.99
Modern	0	Cau 7	380	7.9	8.3	647	0.73	-29.63	21.78	0.68	244	0.62
Modern	0	Cau 8	326	7.6	9.3	728	0.57	-28.35	20.43	0.63	225	0.28
Modern	0	Cau 9	336	8.2	8.8	725	0.67	-29.37	21.50	0.67	240	0.61
Modern	0	Cau 10	368	8.4	8.9	688	0.82	-27.44	19.48	0.59	212	0.53
Modern	0	Caun1	306	8.6	10.4	825	0.60	-27.25	19.27	0.58	209	1.79
Modern	0	Caun2	339	8.6	10.0	853	0.65	-26.55	18.54	0.55	199	1.69
Modern	0	Caun3	292	7.4	10.3	817	0.47	-26.92	18.93	0.57	204	1.84
Modern	0	Caun4	341	8.9	10.8	915	0.72	-26.99	19.00	0.57	205	1.6
Modern	0	Caun5	414	7.7	9.8	755	0.70	-26.73	18.74	0.56	202	2.08
Modern	0	Caun6	297	8.9	10.5	851	0.61	-27.04	19.05	0.57	206	1.68
Modern	0	Caun7	324	8.2	10.0	843	0.63	-26.62	18.62	0.56	200	1.68
Modern	0	Caun8	314	8.3	9.5	792	0.63	-26.98	18.99	0.57	205	1.95
Modern	0	Caun9	324	8.3	10.3	822	0.63	-26.40	18.38	0.55	197	2.16
Modern	0	Caun10	361	8.6	9.9	704	0.75	-26.77	18.77	0.56	202	1.43

Appendix III. Relationship between modeled maximum CO_2 assimilation rate and leaf nitrogen concentration of *Nothofagus dombeyi* samples from late Pleistocene (~15,300 – 13,200 ^{14}C yr BP), mid-Holocene (~6,700 – 4,900 ^{14}C yr BP), and modern time. By applying the linear regression model of Schulze et al. (1994). The scaling of leaf nitrogen concentration to maximum stomatal conductance produced the regression line y=0.3012x, then, the scaling of maximum stomatal conductance to maximum ecosystem surface conductance for evaporation, produced the regression line y=2.996x, and finally, the scaling of maximum ecosystem surface conductance for evaporation to maximum CO_2 assimilation rate produced the regression line y=1.048x.

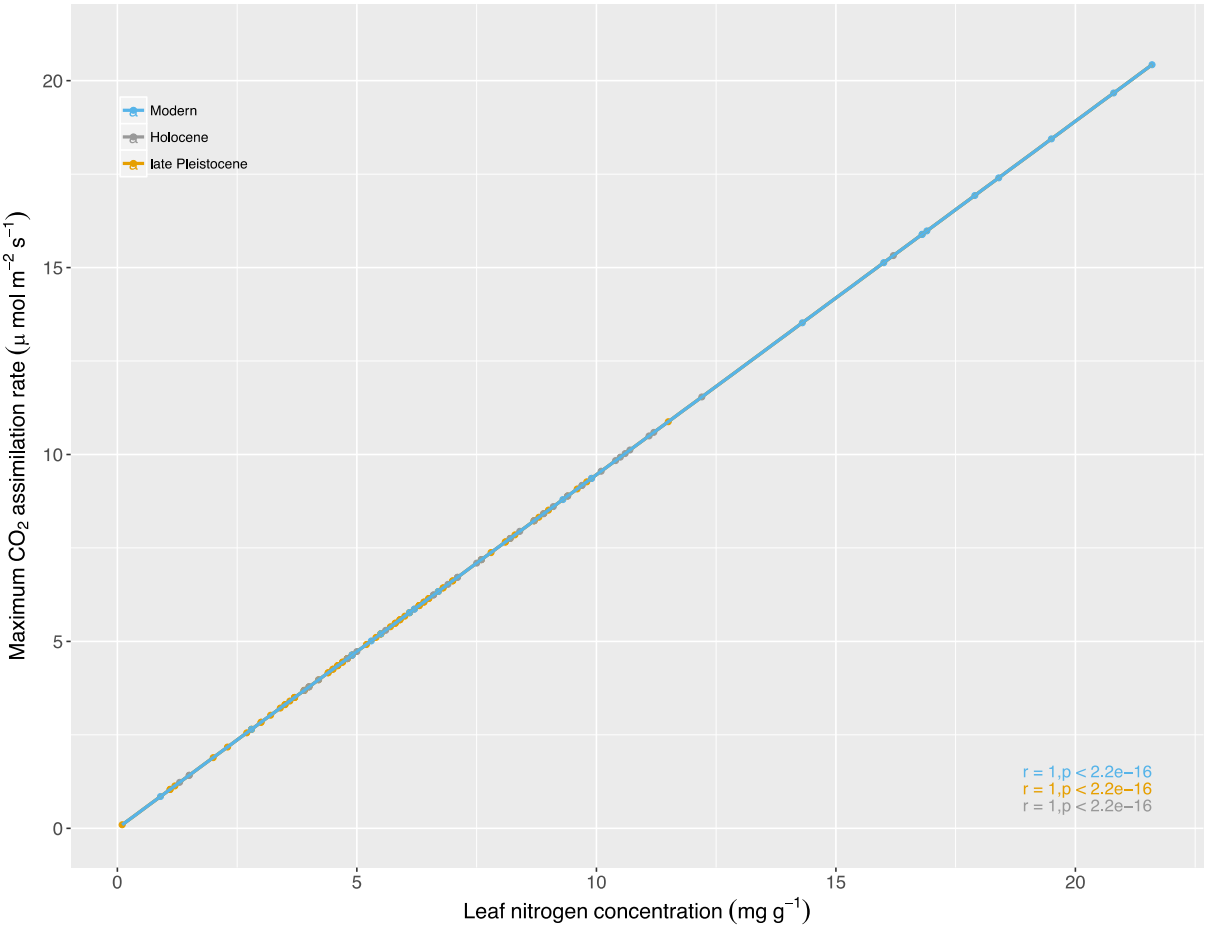

Appendix IV. A) the sensitivity analyses on the photosynthetic rate at a given CO_2 concentration (A_0), and **B)** the scaling relationship between the maximum operational conductance (g_{op}) and the maximum stomatal conductance (g_{max}). The data reveal that a shift in values of the A_0 and g_{op}/g_{max} ratio induced changes in CO_2 estimates from the one hundred and forty *N. dombeyi* samples.

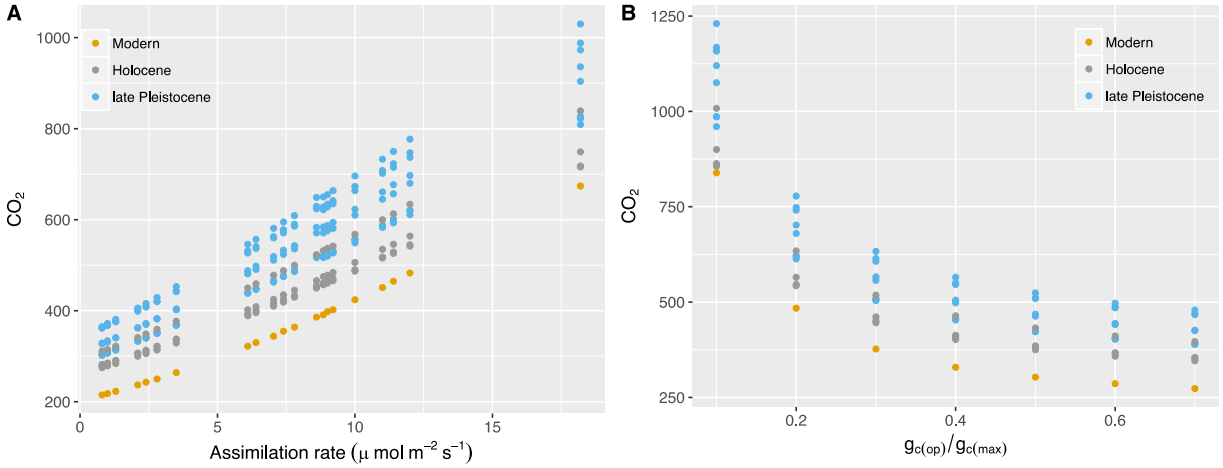

Appendix V. Effect of carbon isotope composition ($\delta^{13}C$) of *N. dombeyi* samples on estimated CO_2 concentrations.